Radiation dose calculation uncertainties on cone beam CT scans of the Ethos radiotherapy machine used for daily adaptation.

Master Thesis

Niels Bohr Institute and Rigshospitalet

University of Copenhagen

Written by

Jonathan Piet Fjeldvig Gammeltoft

Supervised by

Ivan Richter Vogelius [1]

Jens Jørgen Gaardhøje [2]

[1]Oncology department, Rigshospitalet
[2]Niels Bohr Institute, University of Copenhagen

UNIVERSITY OF COPENHAGEN

FACULTY:	SCIENCE
INSTITUTE:	Niels Bohr Institute
AUTHOR:	Jonathan Gammeltoft KU-ID: KGJ652
TITLE:	Radiation dose calculation uncertainties on cone beam CT scans of the Ethos radiotherapy machine used for daily adaptation.
SUPERVISORS:	Ivan Richter Vogelius Jens Jørgen Gaardhøje
HANDED IN:	13th of June 2022
DEFENDED:	22th of June 2022

Radiation dose calculation uncertainties on cone beam CT scans of the Ethos radiotherapy machine used for daily adaptation.

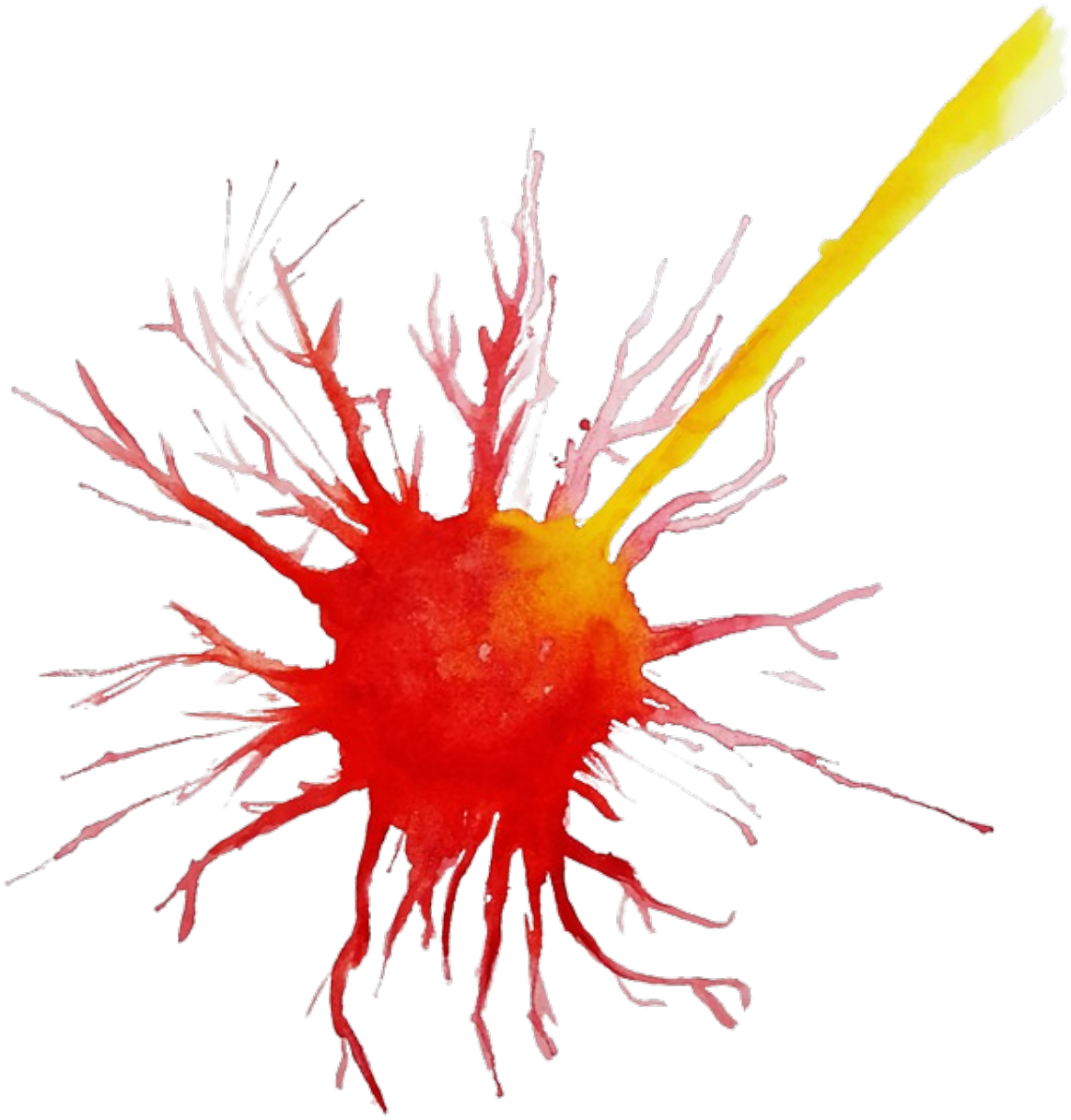

INSTITUTE: Niels Bohr Institute

AUTHOR: Jonathan Gammeltoft KU-ID: KGJ652

SUPERVISORS: Ivan Richter Vogelius
Jens Jørgen Gaardhøje

Abstract

In this project I examined how well adaptive treatment planning holds up over a adaptive planning phase. The objective is to use data from 10 patients treated with adaptive planning. From those treatments sets of cone-beam CTs are made. The sets consists of a CBCT used in the clinic to create an adaptive plan, and a verification CBCT taken after the adaptive flow. By taking the verification CBCT and treat it like a setup CBCT, and creating a new plan in the same adaptive flow. It is possible to see if the time used making the adaptive plan makes it invalid due to waiting time. These examinations are made both at a fraction by fraction level, and as a complete set of all fractions pr patient.

When looking at the fraction by fraction results, it is seen that coverage of CTV50 goes from 97 ± 8 up to 100 ± 0.3 for the adapted plan made from the setup CBCT, and 100 ± 0.6 for the verification CBCT, and thereby showing that for fraction by fraction, the improvement in coverage is greatly improved. When doing an examination across all fractions, we arrive at the same result, CTV coverage is greatly increased, and nothing happen neither positive nor negative to the OAR coverage.

Contents

Introduction

In 1895 Röngten took the first x-ray image of a hand. Already the next year, radiation was used for the time as a cure for cancer. During the early 1900s the technology slowly got better but up through the 19^{th}century oncologists was using the back of their hands to see if their x-ray tube was warm, it took some time for it to be ready, as the filament needed warming. The x-ray tube was ready when the back of the hand became red. That practise ended but it was still the way to treat patients. Wait until the skin became red and then stop. In 1971 the first CT image was taken. And since then the technology have evolved faster and faster. With computer generated treatment plans, the treatment took a huge leap forward, and now a new technology is ready to be tested.
With the Ethos machine it is now possible to take a Cone-Beam CT of the patient while they are lying on the treatment couch. With that possibility it is possible to make changes to a treatment plan based on the anatomy of the day. But how well does it work, and what difficulties does the technology face? That are the questions that I will try to answer in this thesis.

To do that I have split the project up in 3 chapters:
Chapter 1:
Theoretical background - CT-scans, Houndfield unit, electron density and deform image registration.
Chapter 2:
Robustness of adaptive planning.
Chapter 3:
Dose accumulation across all adapted fractions.

1 Chapter 1 - Theoretical background

The theoretical background general for both chapter 2 and 3 will be described in this chapter.
In this general background CT-modalities, dose calculation and deform image registration, will be described. These subjects are needed to understand imaging and dosages described in chapter 2 and 3.

1.1 Dose calculation

Dose calculation is dependent on many things, but mainly the type of radiation, in this case photons, and the electron density of the material, in this case a patient. The energies used for

this type of treatment is the 6MV photons. Meaning We have photon energies up to 6 MeV but the median around 2 MeV, as seen in figure: 1, the main interaction at these energies for carbon, oxygen, nitrogen, calcium and the rest of the atoms that form our body is Compton scattering.

1.1.1 Compton scattering

When we have energies in and around the 2Mev mark, we most often encounter compton scattering. As seen in figure: 1. The main reason to discuss this effect, is that it is the way photons, with these energies, deposit energy in the body.

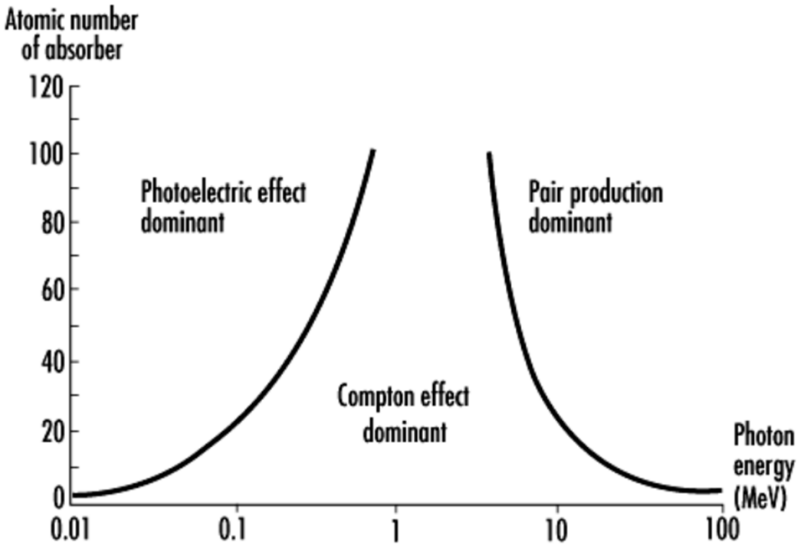

Figure 1: Graph showing the probability of interaction types as a function of photon energy and atom-number, Z.

When a quasi-free electron, an electron with a binding energy much lower than the photon energy, is freed from the atom it interacts with other atoms and electron. In doing so it deposits its energy where it interacts. If the photon energy is very high, the electron will get a large amount of kinetic energy, and the opposite if the photon energy is low. That means a high energy photon, will not only have a large range for it self but will also give the electron a large range.

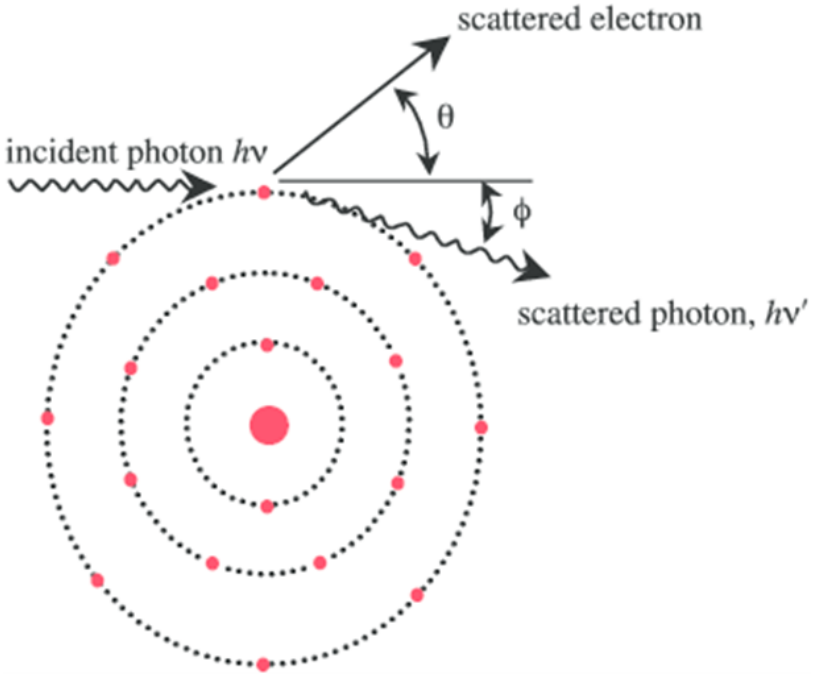

Figure 2: Figure showing how compton scattering works.

1.1.2 Electron density and Houndsfield units

The range of both the photon and the secondary electron, not only depends on their energy, but also on the amount of electrons, the electron density. A higher electron density results in a higher probability for both the initial photon and the secondary electron to interact, and thereby lower their range. Lowering the range is another way of saying that the attenuation is getting higher and therefore a larger amount of energy will be deposited on a shorter range.

Bone, that is primarily calcium Z = 20, has a higher number of electrons and in turn a higher electron density than for example water, Z = 8 + 1 + 1, from oxygen and hydrogen. Bone therefore has a higher attenuation and energy will faster be deposited, or in another way, the penetration power of the photon is lowered in a high density material.

When taking a CT scan electron density is important, and the way to show the electron density, and thereby the density of the different areas in the picture is by using Houndsfield units. Houndsfield units represent a gray scale, with white at larger values and black as lower values, larger values meaning high density, and lower values, lower density.

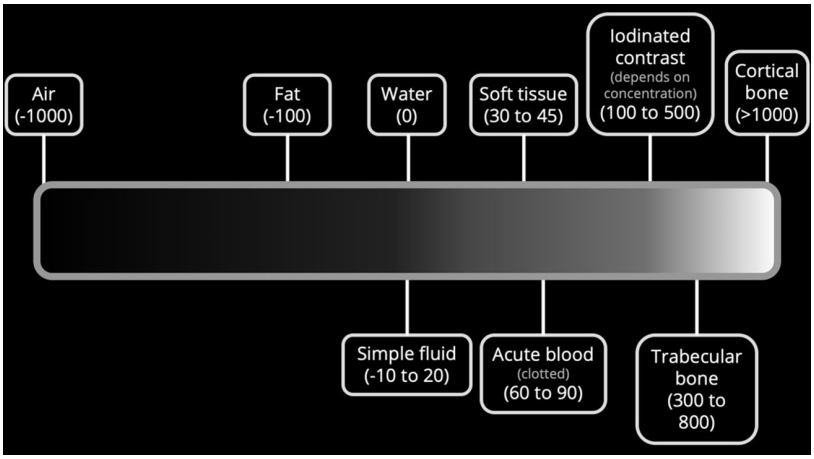

Figure 3: A simplified Houndsfield map, showing different objects and structures and their corresponding houndsfield unit. [7]

When taking a CT scan, we get the full range of houndsfield units, but that would be useless to look at due to lack in contrast. Therefore in order to look at a CT scan, a houndfield unit window is chosen. Choosing different windows will result in contrast between different objects. A small window at values around the soft tissue values presented, will blur out any details in bone structure, making everything bright white, but it will increase the contrast in the soft tissue, making it easier to notice the difference between different soft tissue structures. So choosing the houndsfield unit window is important when choosing what to look at.

1.1.3 The Boltzmann transport equation and Acuros - the dose calculation algorithm

The Boltzmann transport equation is a set of equations that describe how different particles travels through matter. A special case of these equations is the linear Boltzmann transport equation, LBTE, and is under the assumption that under the transport through matter, the particles only interact with the matter particles and not with each other. This assumption hold if there is no external magnetic field. [2].

In Eclipse, the planning tool used to calculate dose, there is a dose calculation algorithm called Acuros.
The Acuros algorithm uses the following formula, the LBTE, to calculate the dose deposited in tissue.

$$D_i = \int_0^\infty dE \int_{4\pi} d\hat{\Omega} \frac{\sigma^e_{ED}(\vec{r}, E)}{\rho(\vec{r})} \Psi^e(\vec{r}, E, \hat{\Omega}) \tag{1}$$

Where D_i is the dose deposited in the i^{th} voxel, E is the photon energy, Ψ^e is the angular electron fluence. Electrons not being the primary radiation, but almost all deposited energy comes from

secondary radiation of electrons. $\hat{\Omega}$ is the direction of the electron fluence. Those variables depend on beam energy, type of machine and more factors, and are defined in the algorithm they are therefore unknown to me. The fraction in the middle consist of: $\sigma^{e}_{ED}(\vec{r}, E)$, the macroscopic electron energy deposition cross section in units of MeV/cm and $\rho\vec{(r)}$ the density of the material in units of g/cm^3. That fraction gives the total attenuation in units of cm^2/g, and is highly dependent on electron density and is therefore correlated with houndsfield units in any given volume.

1.2 Deform image registration

To to deform image registration we need to follow the chart in figure: 4:

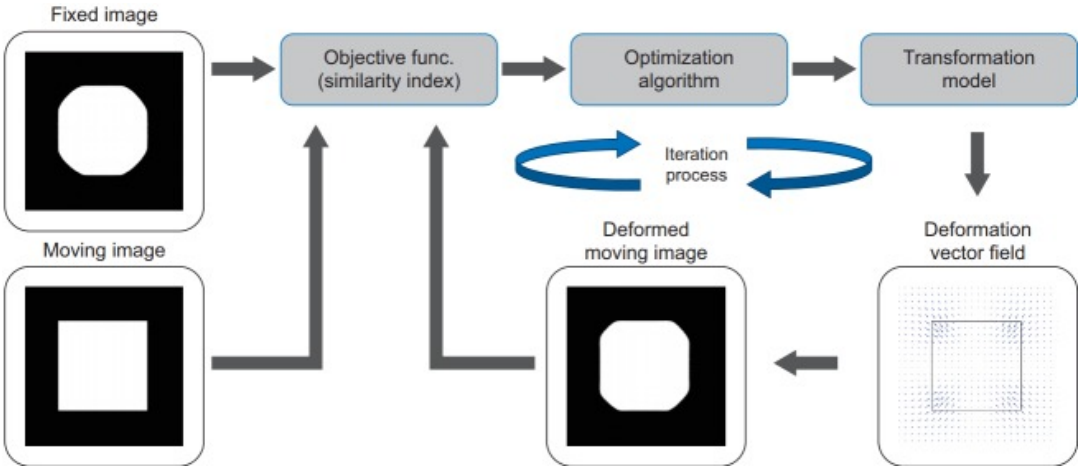

Figure 4: Step-by-step description of how image deformation works. Step 1: A fixed image, the image you want to deform to, and a moving image, the image you want to deform, is chosen. Step 2: Using an similarity function, the two images are compared. Step 3 and 4: An optimization is made and a model describing how that optimization is done is also generated. Step 5: A deformation vector field is generated, telling how the moving image is changed. Step 6: Deform the moving image. Step 7: Return to step 2 and repeat until similarity is reached. [6]

The similarity function is based on the Sum of Squared difference:

$$SSD = \frac{1}{N} \sum_{x' \in \Omega} [I_F(x) - I_M(x')]^2 \tag{2}$$

Ω is the number of overlapping voxels between the fixed and the moving image. N is the number of voxels in Ω, $I_F(x)$ is the intensity of the fixed image and $I_M(x')$ is the intensity of the moving image. All in all this gives us that when SSD approaches 1 the two images are similar.

1.3 CT modalities

To compare the conventional-CT, CT, method with the ConeBeam-CT, CBCT, it is first important to describe each of them. In the following CT and CBCT will be described and compared. These

methods or modalities have each their own strengths and weaknesses that are utilised during a radio-treatment setup. These strengths and weaknesses will also be described and compared. Thereafter synthetic-CT will be described, as these pictures are build from other types of CT or MRI, in this case from the CBCTs.

1.3.1 Conventional CT

A CT-scan, is an imaging technique with a great soft-tissue to bone contrast [5], but with lower soft-tissue to soft-tissue contrast than MR. When viewing a larger field, and functionality is not the main concern a CT, can, and often will, be chosen as the imaging modality. And especially when looking for, or planning a treatment for a tumor a CT scan is most often chosen [8].

A CT scan is essentially a 3D x-ray, build from 2D images from many different angles. The theory behind a CT-scan with i focus on how the image is generated will be described in the following:

In order to have a viewable image several steps needs to be taken.

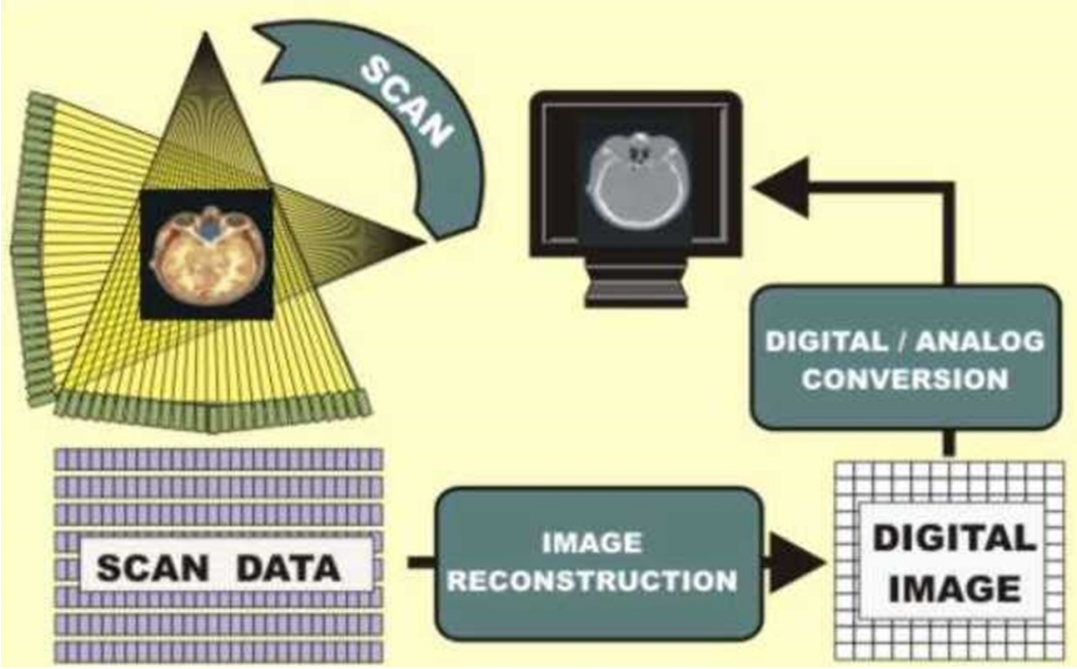

Figure 5: Step-by-step description of how a CT image is made. [13]

Firstly the scan itself:
Earlier parallel or single x-ray beams, called pencil beams, where used in order to take the image, but since 2000 we most often use the fan beam technique, especially due to lowered exposure to dose and faster scan time. On the other hand a pencil beam will give the option of spare some organs or areas that should not have any radiation due to a higher accuracy of the beam.

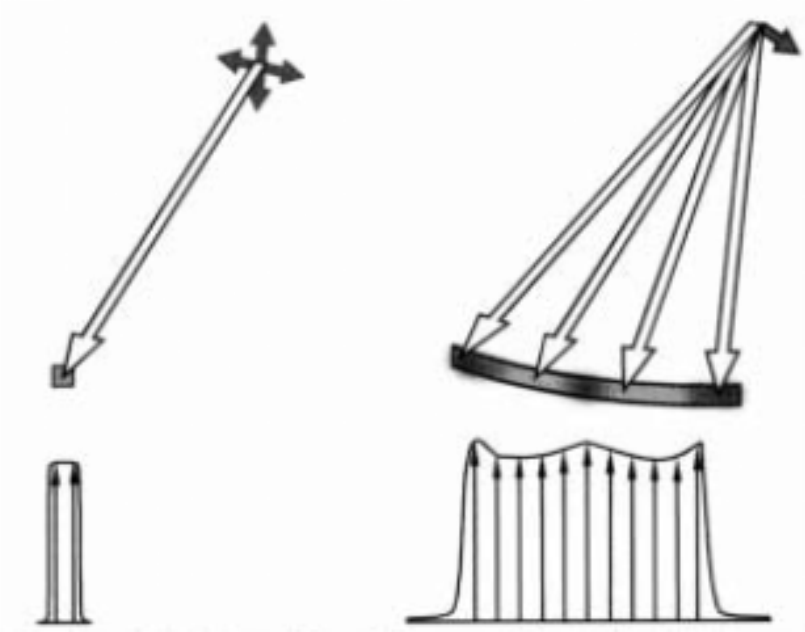

Figure 6: Illustration showing the difference between pencil beam delivery and fan beam delivery. Both setup and intensity at detector (without any patient or other media between source and detector). [1]

As seen on figure: 6, the intensity of the pencil beam is more box-shaped, resulting in a, as stated, very high accuracy, but a longer scan time. And a longer scan time results in more time for the patient to move and thereby increase the uncertainty of the scan, even though the technique itself is of higher accuracy.

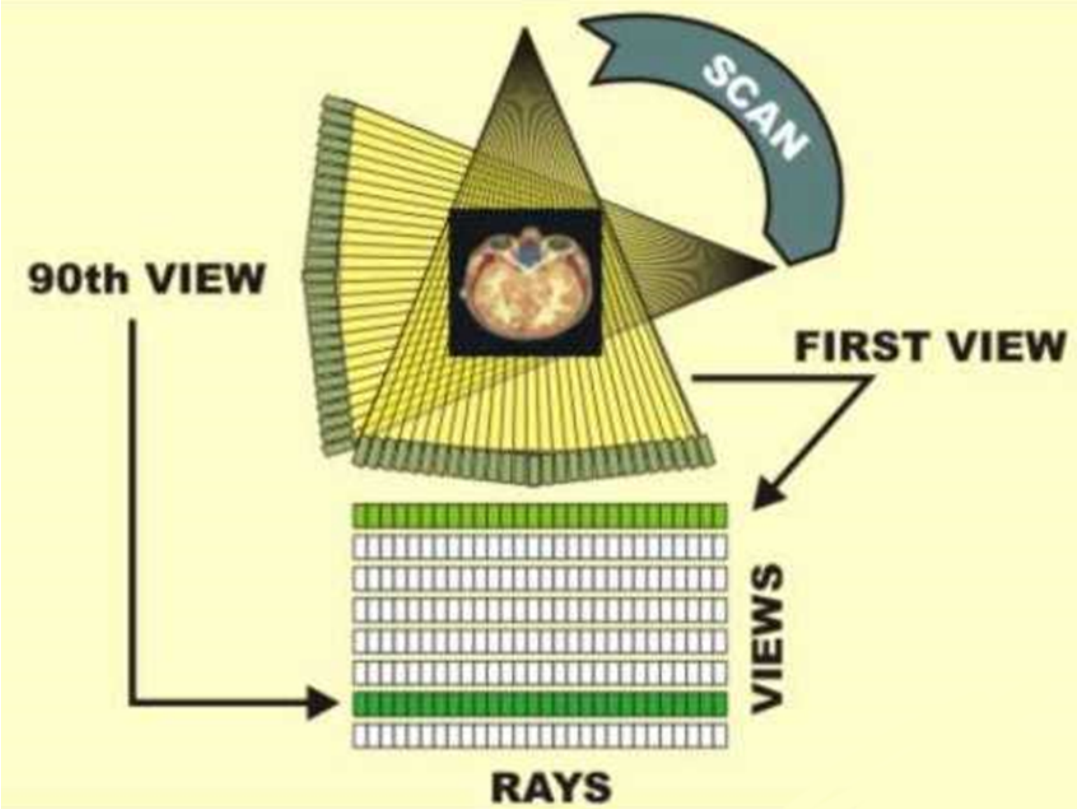

Figure 7: Illustration showing how view angles are translated into a data file. The x-axis ”Ray” gives the number of detectors and what that detector measured as a function of view angle, described by the y-axis. [13]

A way to describe the data measured by the detector would be to set the value measured at each detector, if nothing was between the source and the detector, to 100%. And then when the patient is introduced, the new value measured would give an idea of the total attenuation between the source and the detector. That gives us, for each ”View”, a set of percentages, a data set.
With enough ”views” it is possible to generate a picture using a technique called back-projection, or better yet, filtered back-projection, which will be explained in detail later.
When taking a series of ”views” and building up a data set and that results in one slice, one single image, the technique is called Step-by-step, as shown in figure: 8.

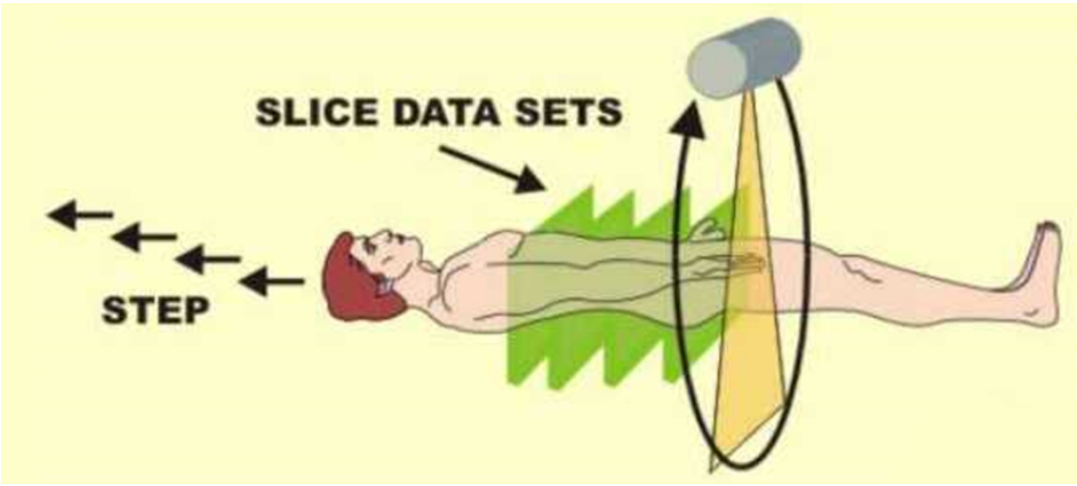

Figure 8: Illustration showing how step-by-step scanning results in discrete slices defined by step length. [13]

When using this technique each data slice is defined by how far into the scanner the patient is. And in order to make a 3D image a lot of slices are taken. The resolution, between slices, of the 3D image is the result of the distance the patient was moved between each slice. That results in some restraints, such as:
After the scan is taken and the patient is out of the scanner there is no way to see ”between” the slices, the scan is not continuous. The thickness of each slice is also fixed, and is defined by the equipment.
In order to combat these restraints helical scanning is used.

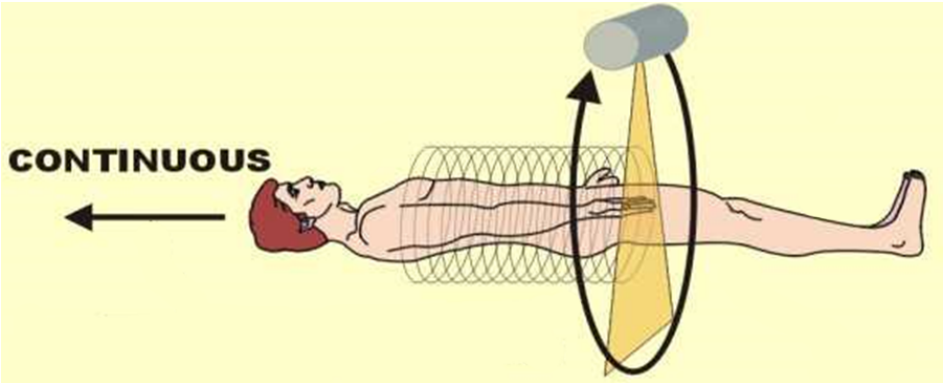

Figure 9: Illustration showing how view angles are translated into a data file. The x-axis ”Ray” gives the number of detectors and what that detector measured as a function of view angle, described by the y-axis. [13]

As it can be seen in figure: 9, the helical scanning is continuous, that means it has the potential of a continuous image. A continuous image is one where the slices are overlapping and it is possible to define slice thickness and separation points in the computer, and more importantly it is possible to change these separation points and thereby, depending on pitch, as explained below, be able to take a full image without any loss of information between slices.
In order to get this continuous pictures the pitch value chosen will be important.

Pitch is defined as: The distance the couch travels pr rotation divided by the width of the slice, as seen in equation: 3. The couch is the plane the patient lies on, and rotation is referring to the x-ray source and as such the detector doing a full revolution around the patient.

$$P = \frac{D}{W} \tag{3}$$

Pitch value is a way of describing the helical scan. A pitch value of 1 is when the slice thickness and the couch distance are equal to each other, that results in a scan with total cover of the patient with no overlapping zones of the slices as seen in figure: 10.

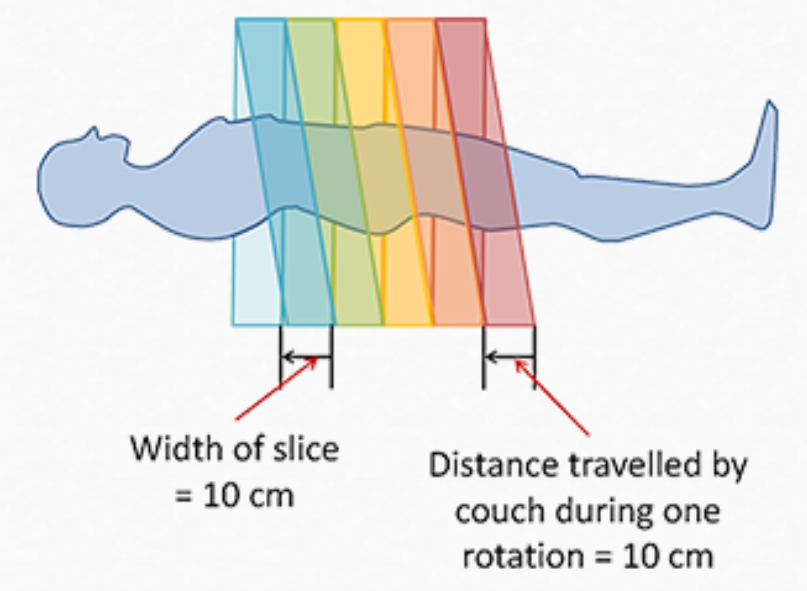

Figure 10: Illustration showing, Pitch = 1. [9]

Pitch values > 1, means that the couch travels a longer distance than the width of the slice, as seen in figure: 11. This result in lower resolution depending on how much larger than 1 the pitch value is but at the same time results in a lower dose, and a shorter scan time.

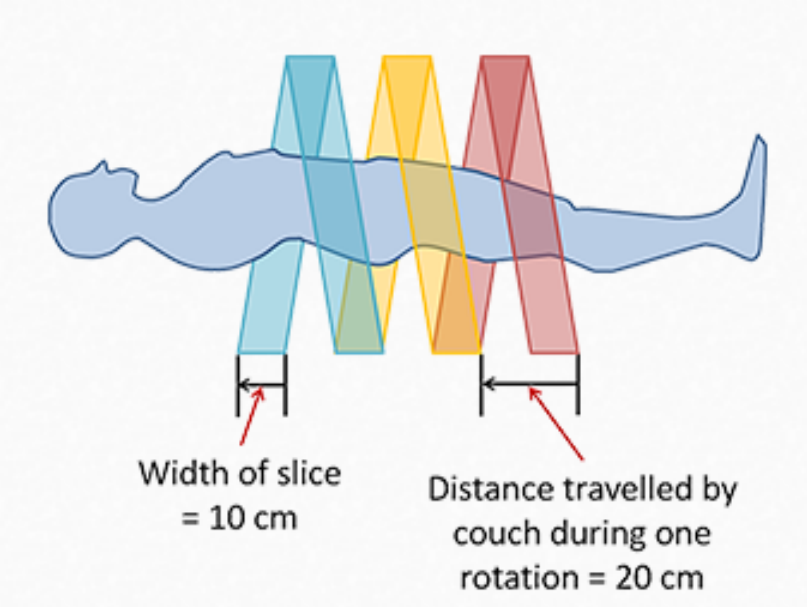

Figure 11: Illustration showing, Pitch = 2. [9]

Pitch values < 1 means that the couch travels a shorter distance than the width of the slice, as seen in figure: 12. This results in a higher resolution but increases scan time and dose to the patient.

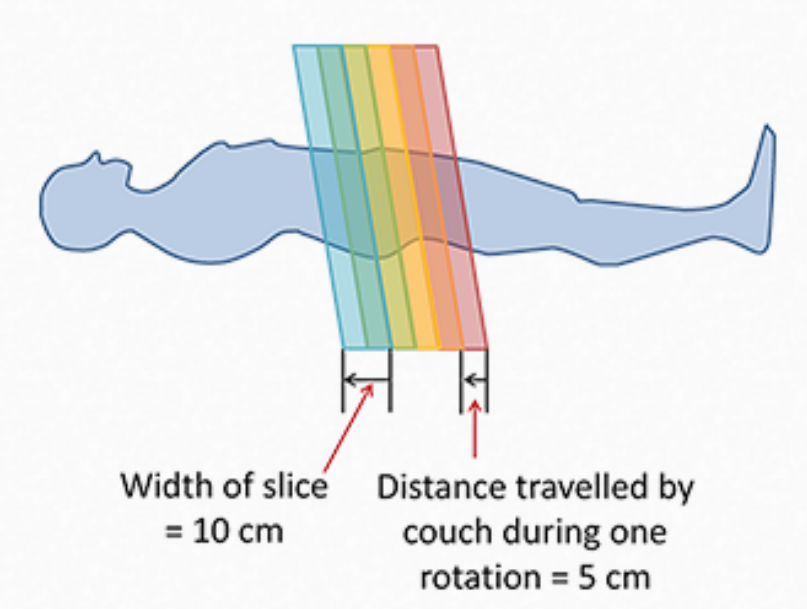

Figure 12: Illustration showing, Pitch = 0.5 [9]

As shown, different pitch values has different properties. Pitch values of over 1.5 are rarely used due to low resolution, and similarly low pitch values are rarely used due to high dose to the patient. Pitch value is chosen based on importance of the resolution of the image compared to the dose allowed to the patient. A lower pitch value can more easily be chosen if the target volume is small due to the inherently lower total dosage. Similarly a higher pitch value is chosen for a larger volume.
When the image is taken, the data needs to be converted into an image file that can be viewed. The most common conversion is the filtered back projection.

Filtered back projection

In order to understand back projection and in turn filtered back projection we firstly need to understand forward projection.

In figure: 13, a table with measured pixel values from a CT scan is shown.

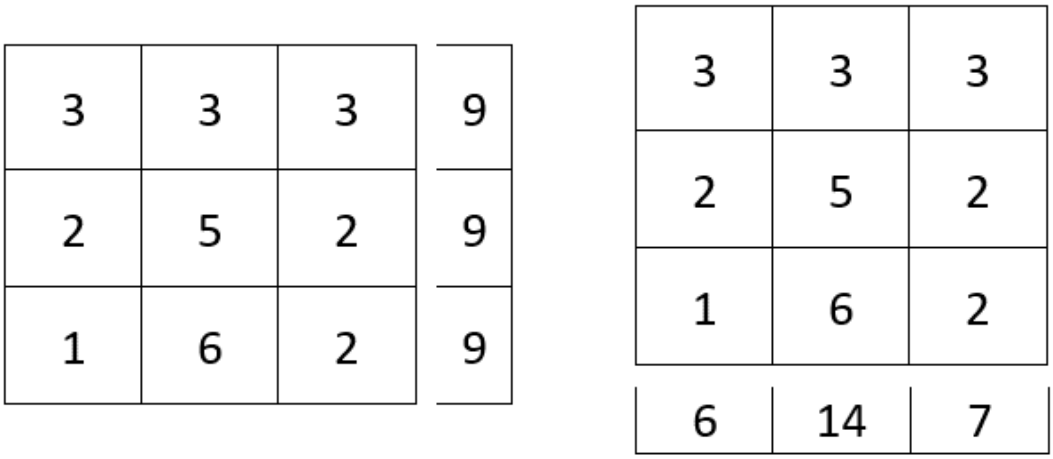

Figure 13: Table on the left showing adding pixel values horizontally. Table on the right showing adding pixel values vertically.

The column and row to the right and below the tables show the sums of the pixel values in the corresponding rows and columns. When doing forward projection, information about how the data is spread out is lost. In order to combat the loss in information multiple angles are used. As seen in figure: 13, when doing the forward projection from several angles, we increase the information gained for each pixel.

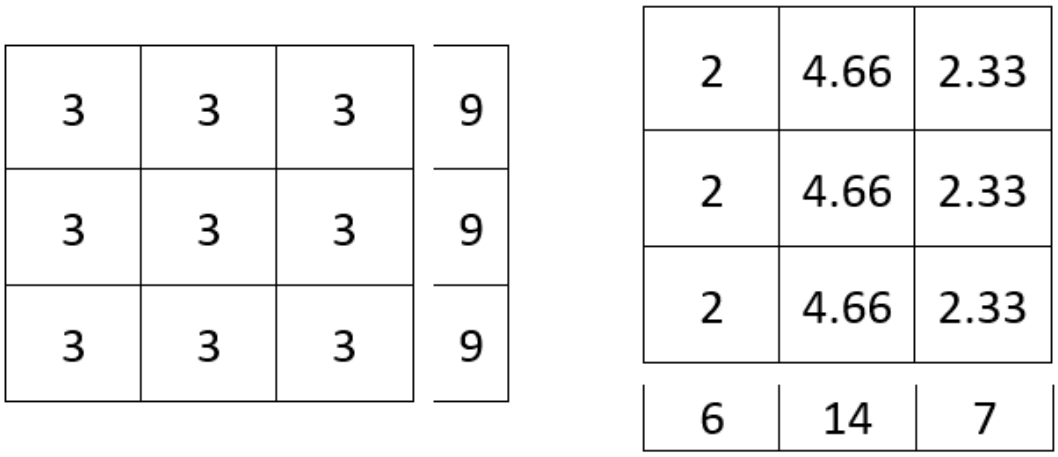

Figure 14: Table on the left showing back projection of values from the forward projection, horizontally. Table on the left showing back projection of values from the forward projection, vertically.

Back projection, as seen in figure: 14, takes the sum from the forward projection and spreads it equally out across all pixels that contributed to the sum. When doing that, the loss of information from the forward projection becomes apparent. In order to overcome the loss of information multiple angles are used, and as seen in figure: 15, an average of the two back projected tables is made. This average comes closer to the original measured values, compared to any of the two back projected tables by them selves. So in order to further increase the likeliness between the average back projected data and the original, more angles, and thereby more unique information is retrieved.

2.5	3.83	2.66
2.5	3.83	2.66
2.5	3.83	2.66

Figure 15: Table showing the average values from both the vertical and horizontal back projection.

But no matter how many angles used, the data will still be smoothed out compared to the original, meaning that the resulting image will lack edges and general resolution. An example of this effect can be seen in figure:

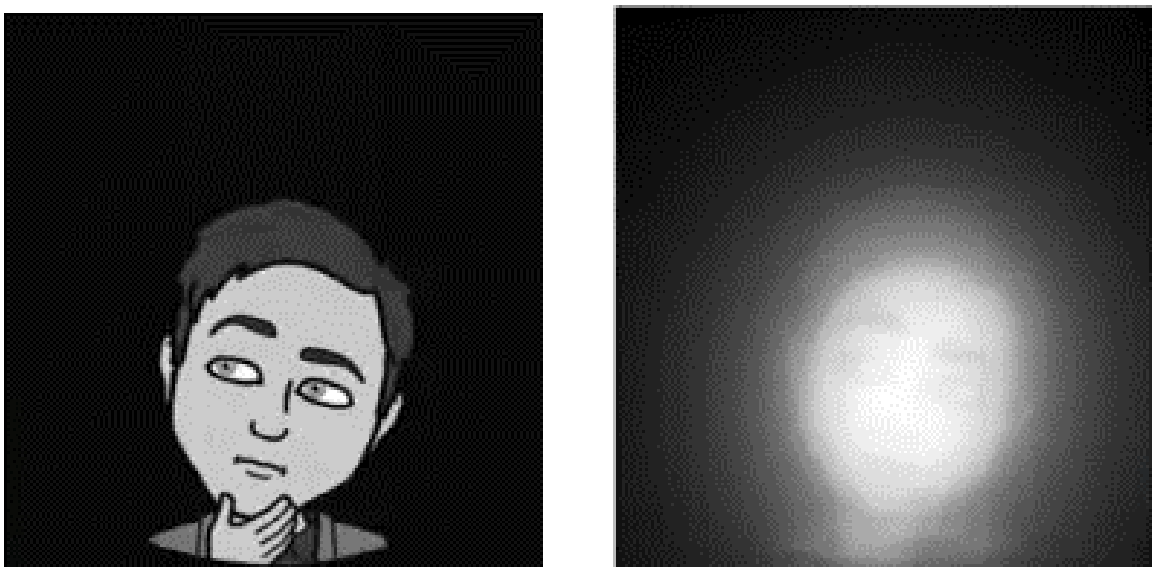

(a) Original object (b) Back projection without filter

Figure 16: It is clear here to see that the resolution goes drastically down when using back projection without a filter[10]

In order to combat this effect we come to filtered back projection. To apply the filter a sinogram is created.

Figure 17: A sinogram made from a scan of figure: 16a. Horisontal lines in the sinogram is made from a single viewing angle. The vertical dimension is then created from many viewing angles. [10]

The filter most often applied is the Ram-Lak filter, this is a filter that enhances the edges of the original image, by enhancing the pixels with a lot of information and decreasing the pixels with a low amount of information. Thereby reducing noise and the blurred effect shown in figure: 16b.

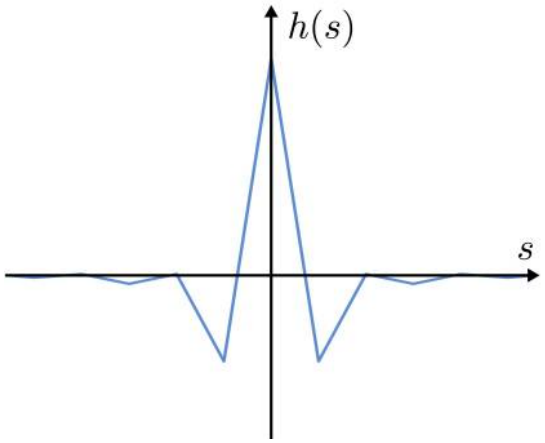

(a) The Ram-Lak filter in the spacial space, where s is a point along the sinogram x-axis, which is where we will apply the filter. h(s) is the filter strength

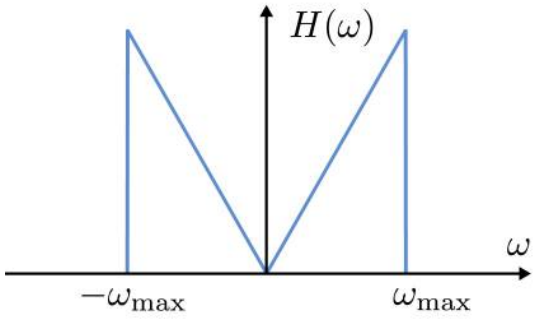

(b) The Ram-Lak filter in frequency space, where H(ω) is the filter strength at given frequencies. It should be noted here that th Ram-Lak filter in the frequency space is a highpass filter, due to high frequencies are responding to edges in the spacial space.

Figure 18: Comparison between the frequency space and spacial space for the Ram-Lak filter. [11]

When applying the filter on the sinogram of figure: 17 it is done on the Fourier transposed sino-

gram, and thereby applying the highpass filter, and then converting back to the spacial space. When that is done we get the following sinogram, figure:

Figure 19: Sinogram in figure: 17, after application of the Ram-Lak filter. [10]

After application of the Ram-Lak filter it is clear to see the edges in the sinogram more clearly. Now we are ready to do the back projection again, on the filtered sinogram:

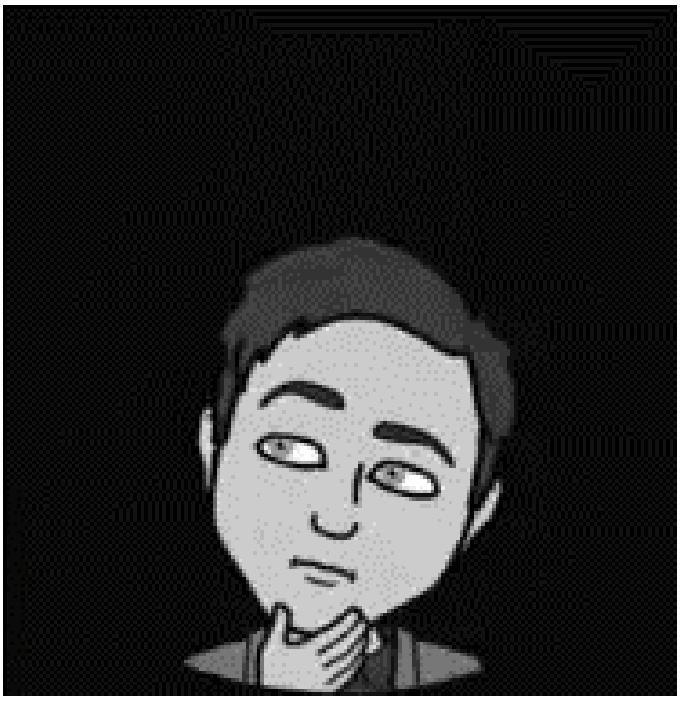

Figure 20: After the filter has been applied it is clear to see that the noise is filtered and the edges are much more clear. [10]

As it can be more clear to see in a simpler example, I apply the same Ram-Lak filter to a simple

dot, figure: 21

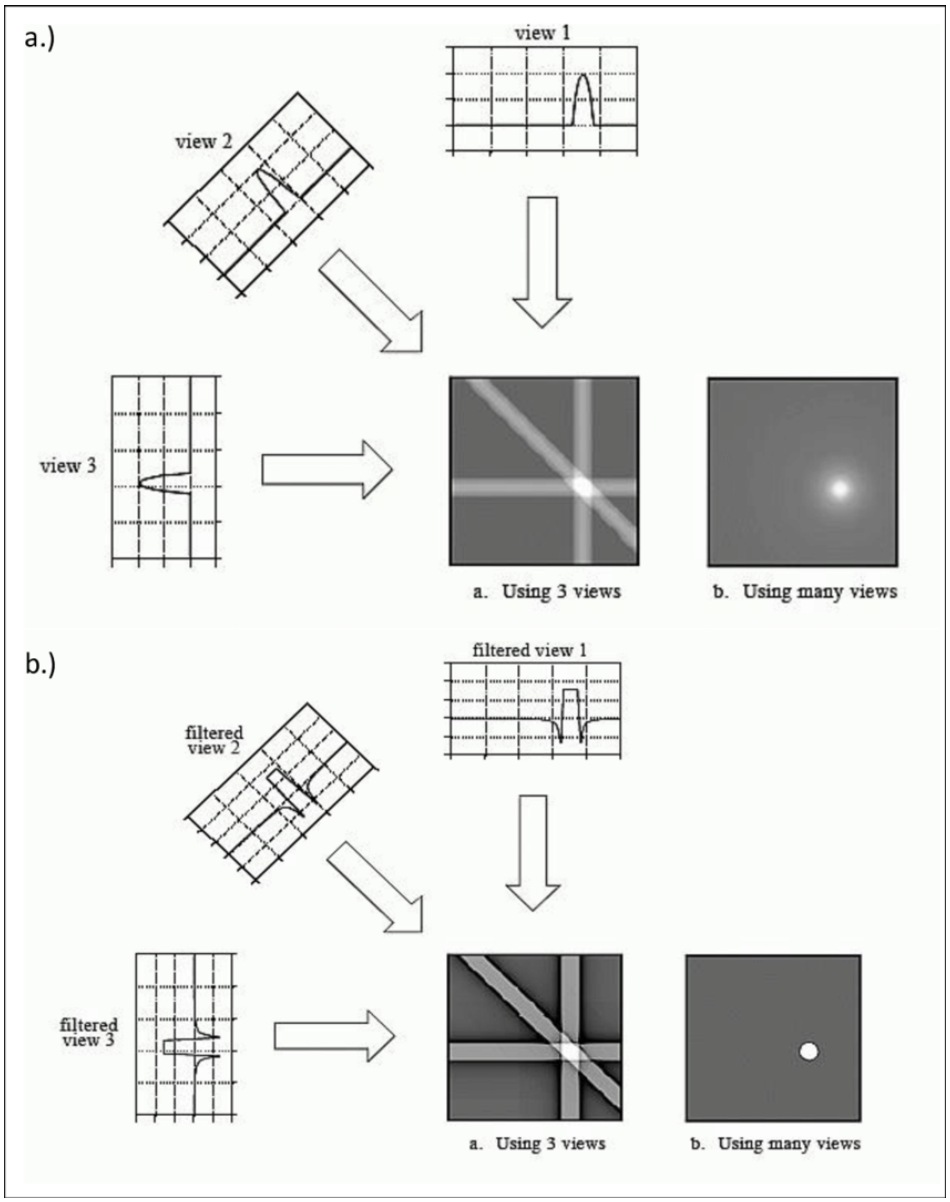

Figure 21: Part a, a) Showing back projecting without filtering from 3 angles, views. Part a, b) Showing unfiltered with many views, and as seen here it gets blurred and edges are not well defined.
Part b, a) Showing the 3 angles, this time with a filter enhancing edges. Part b, b) Showing many angles with sharp edges due to filter being applied. [4]

1.3.2 ConeBeam-CT - CBCT

Cone-beam CT, CBCT, is a fast CT technique where the x-rays diverge from a point source into a cone. By being a cone the CBCT has a large image area, and can therefore take images very quickly, with limited dose to the patient. Dependent on the field size it is often possible for a CBCT to take a complete image with only one rotation around the patient. Only needing one full rotation limits artefacts from patient movement, both involuntary and controlled by the couch. But due to the cone shape a larger amount of scattering takes place, especially near the sides of the cone. This unpredictable scattering gives rise to houndsfield unit maps of low quality,

thereby planning on these scan is no preferable.

Synthetic CT - sCT

To overcome this bad houndsfield unit map, a synthetic CT is created. A sCT is made by transferring the original houndsfield map from the original CT, to the new CBCT, using deform image registration. By doing that, we get both a fast image and a good houndsfield map, so from that sCT it is possible to create proper dose matrices.

2 Chapter 2 - Robustness of adaptive planning

2.1 Introduction

As of 2020, 362533 danish people lived with cancer. Of those only 0.3%, 1100, had vulva cancer. But it is nevertheless a type of cancer that people are dying from and therefore it must be part of research, in order to increase the number of people surviving the disease, and at the same time lowering their long term complications.

When diagnosed with any type of cancer and then being recommended for radiation treatment, a treatment plan needs to be made. A treatment plan is comprised of a series of scans on which a radiation plan is made. The plan tells at which energies and which angles the radiation must be given. For most types of vulva cancer, we at Rigshospitalet, treats with 27 fractions. That is 27 days the patient must arrive at the hospital, and in most cases get the same treatment everyday. In order to adjust for interfractional anatomical changes, it is normal to set the PTV margin from the CTV to 7mm. These 7mm also accounts for patient movements during treatment.
But with the Ethos radiotherapy machine it is now possible to take a CBCT of the patient, in the same machine as the the treatment will be delivered. This gives us the possibility of making minor adaptions to the treatment plan, and thereby maximize dose to the target area, whilst keeping the dose to the OARs unchanged.
The reason for checking robustness of the adaptation is the time spend on the adaptation itself. The adaptation takes, as a median value, 15 minutes. And during those 15 minutes changes in anatomy can take place. What the consequences are of those anatomical changes to the dose delivered to the CTV and OARs, is examined and via that the validity of doing the adaptation is checked.

2.2 Methods

For this examination we had a total of 10 patients, 252 total fractions all of which underwent adaption on the Ethos accelerator, though for only 60% of the fractions the adaptation were chosen, as the treatment for the patient. Patients will be enumerated 1 through 10, throughout the

rest of the thesis, numbering will stay consistent, so patient 4 will stay patient 4, this will stay true in chapter 3.

The main task while creating a treatment plan is to irradiate the target while protecting the Organs at Risk, OARs. The collective name for any OAR, or target is structure.
The target is split up in three different volumes. [3]

- **GTV - Gross Tumor Volume**
  The GTV is the tumor volume visible on scans and visibly involved lymph nodes. It is the smallest volume of the three.
- **CTV - Clinical Target Volume**
  The CTV is the area around the GTV where it is plausible to find tumor cells that do not show up on scans, being too small to see. In an ideal situation this volume would be the only volume necessary to irradiate.
- **PTV - Planning Target Volume**
  The PTV is a volume around the CTV used to ensure that the dose wanted in CTV is delivered, even though there are uncertainties, in positioning of the patient, the patient moving and breathing, and in the calculation of dose distribution in the patient.

Sufficient coverage of the CTV will be a significant success criteria of the examination, thus PTV will not be used for any of the examinations throughout the data processing.

2.2.1 Workflow of adaptive treatment

In order to understand the data generated for the thesis, we first needs to understand the clinical workflow.

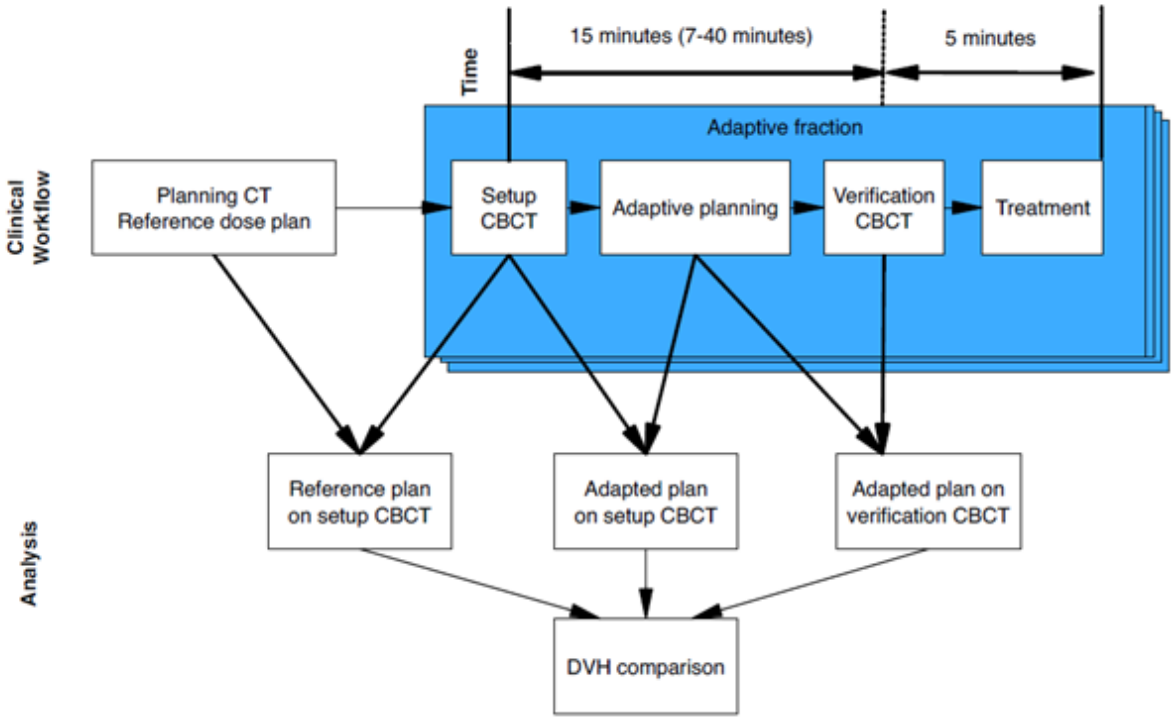

Figure 22: Illustration showing the clinical workflow, the time scale, and the data retrieval for the robustness test. [12]

As seen in figure: 22, the first thing done is that the patient gets a planning CT, this happens before the treatment begins, and is used to build the original plan. We need the original plan in case the adaptation does not improve on the daily treatment, which happens often. In order to do adaptation, a 12 equidistant IMRT field was used for all patients. VMAT was not chosen, even though it is most often used for this type of cancer due to a longer calculation time in the adaptation workflow.

The daily treatment started with patient placement and a CBCT, called Setup CBCT in figure: 22. Using deform image registration, as explained in chapter 1, target and normal structures were displaced from the planning CT to the setup CBCT. After the structures was moved from the original plan, a specialist gynecological radiation oncologist reviewed, redrew and approved the structures, based on the CBCT for the day.
Then two plans were made on the new structure sets. The first plan, the ”scheduled plan on the setup CBCT”, figure: 22 was the dose distribution from the reference plan. It was placed on the new structure set with the deform image registration algorithm. The second plan the ”adapted plan on the setup CBCT”, figure: 22 had the Houndsfield unit map transferred and used as the electron density map, so a new dose distribution could be made.
From these two plans, the physician and the physicist chose the best plan. The best being the plan that covered the target best and at the same time, did not over irradiate the OARs, if no improvement was gained the scheduled plan was used. This adaptation flow took, as a median

value 15 minutes. A more comprehensive overview of the time spend can be seen in the result section.

Just before treatment a new CBCT was taken, the verification CBCT. The verification CBCT is taken in order to be able to make a plan that show how the anatomy has changed, if at all, during the adaptive planning phase. These planned is made in an Emulator so the workflow matches the original workflow as similarly as possible. Patient 5, had an extended CBCT, due to the location of the tumor. The emulator could not make a plan for the extended CBCT patient. This results in patient 5 being omitted from allt result both in chapter 2 and 3, that comes from the plan and not the questionnaire.

That leads to the analysis part of figure: 22. The ”adapted plan on the verification CBCT”, figure: 22. The verification plan is used to check if anatomical changes that took place during the adaptation phase has altered the quality of the adapted plan. The final box in figure: 22, DVH comparison, is the data used to compare if the changes were significant or not.

2.3 Results

Coverage of CTV by mean D95%, D95% being the dose that at least 95% of the target volume is planned to recieve, was $97 \pm 8\%$, for the scheduled plan. But for the adapted plan on the setup CBCT that value was $100 \pm 0.3\%$ and on the verification CBCT $100 \pm 0.6\%$. This shows a significant improvement of coverage with both a higher percentage of the volume getting the required dose and a lower uncertainty, and most important it is shown that the improvement is kept during the adaptation process.

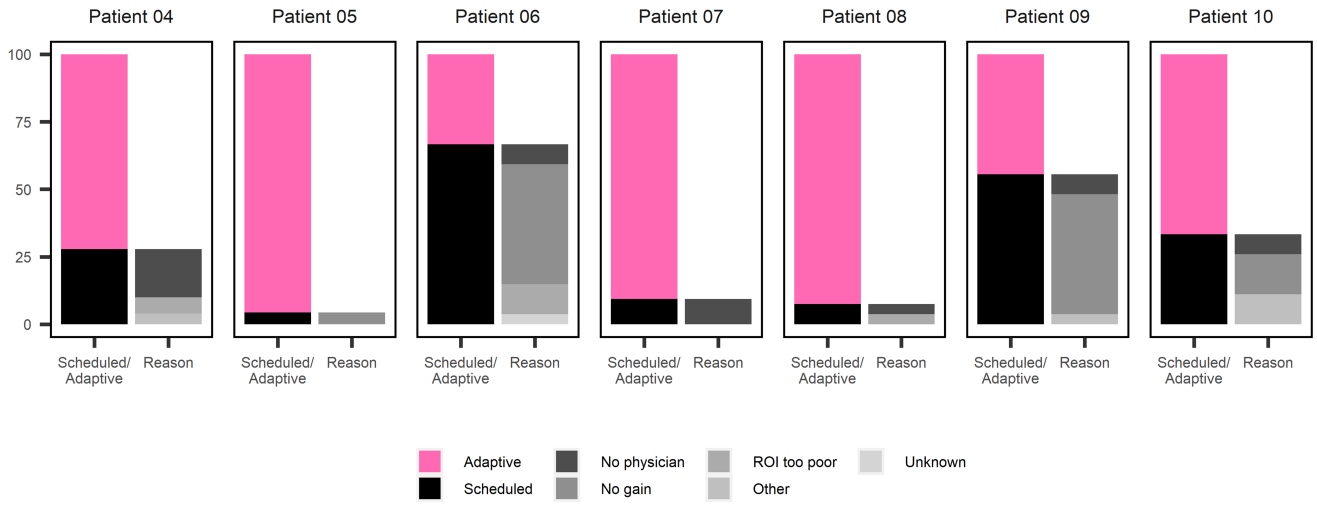

Figure 23: Showing patients, and whether or not the adapted plan was chosen. If not reason for that is also shown. Patient 1-3 is not shown here due to this data being based on a questionnaire filled during or immediately after treatment by the doctor, and the questionnaire was only implemented after patient 3. The few fractions where the reason for choosing the scheduled plan is unknown, are fractions where the doctor did not fill out the questionnaire. [12]

From figure: 23, we know that out of the 252 fractions, 150 fractions were adapted. The main reasons as to why the scheduled plan was chosen was ”no significant dosimetric gain” - 29 fractions. When no dosimetric gain is accomplished, the scheduled plan is used due to it being made on a better scan with time to do make the plan. The second main reason was that ”MD not available for treatment”, when no doctor is present there is no one to redraw OARs, and no one to approve the new plan, therefore this will always be the scheduled plan.

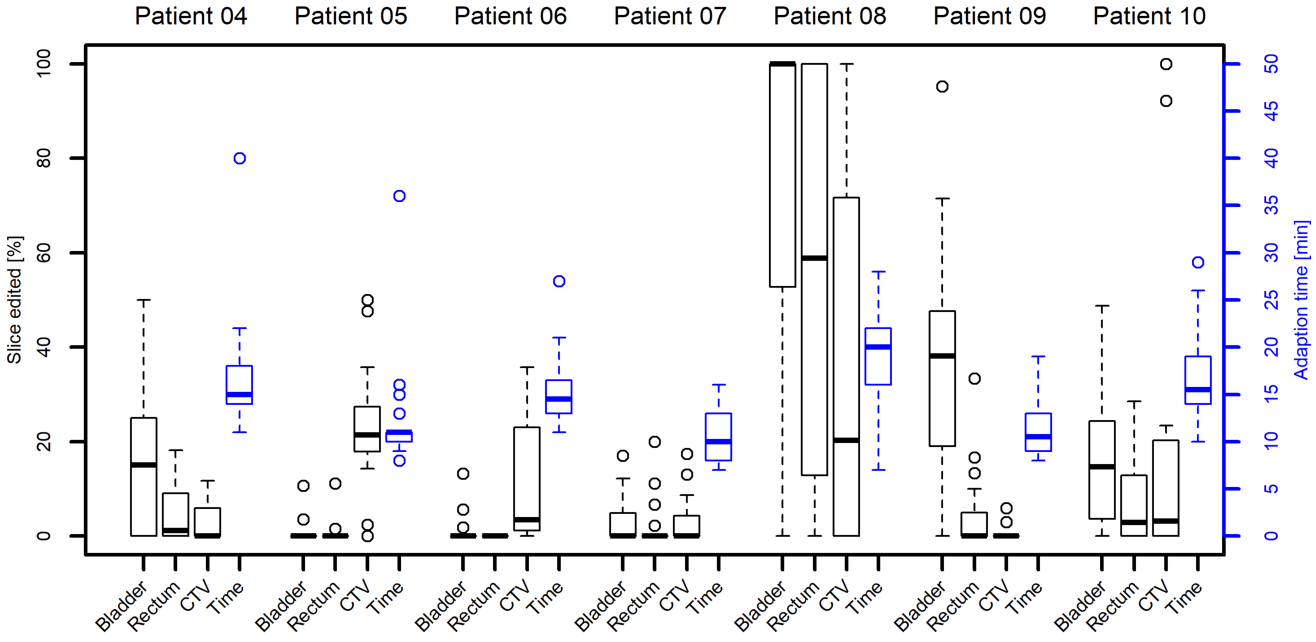

Figure 24: On the x-axis the structures, bladder, rectum and CTV are defined, we also have a time slot for every patient. By ”time” we mean time spend in the adaptation step of the procedure. On the left hand side y-axis we have the fraction of slices edited. And on the right hand side y-axis the adaption time in minutes can be found. Again only patient 4-10 due to the questionnaire. [12]

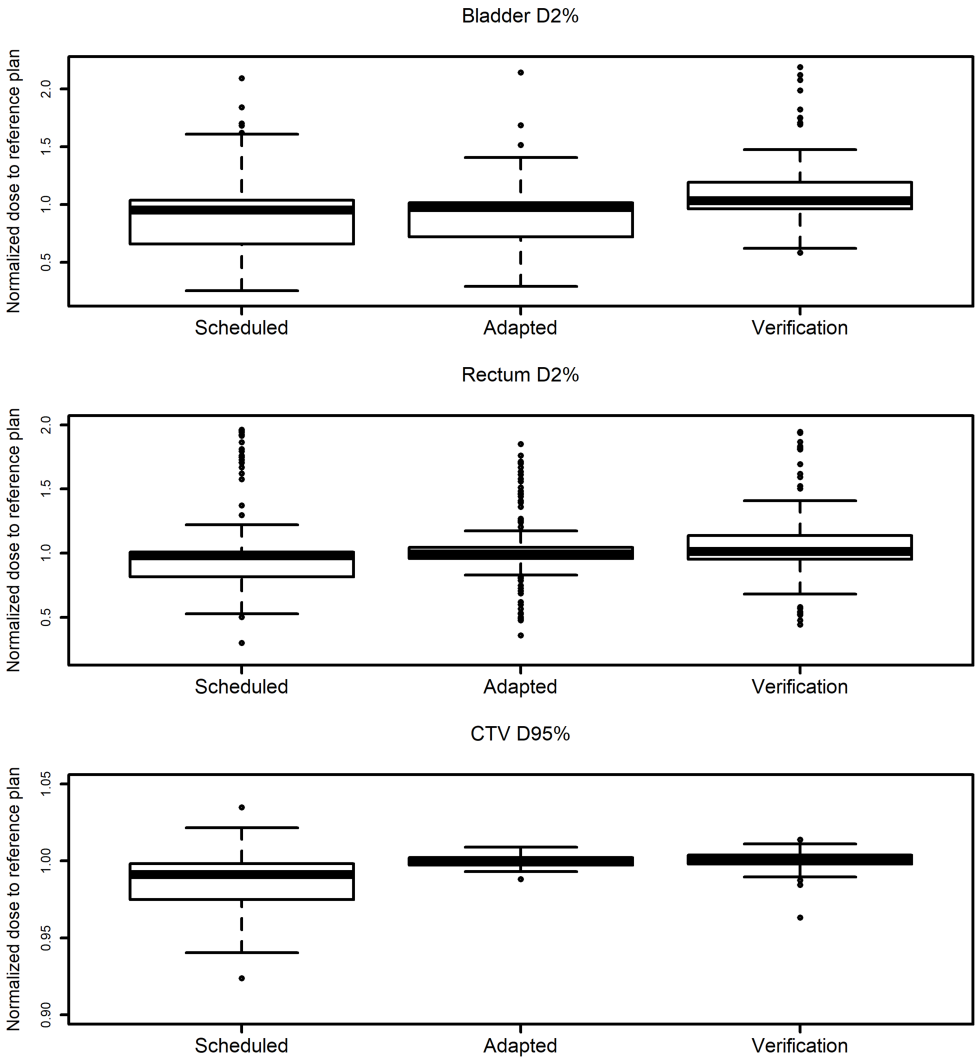

Figure 25: Three box-plots comparing the scheduled, adapted and verification plans. The first compares bladder $D2\%$, the second rectum $D2\%$ and the bottom one CTV $D95\%$. This plot is based on [12]

$D2\%$ being the hottest 2% of the bladder, hottest meaning the volume that receive the most radiation. As an OAR it is preferable to keep the radiation as low as possible, therefore values under the dose normalized to 1 is good. Similarly for the rectum.
CTV $D95\%$ is defined as the minimum dose at least $D95\%$ of the CTV should receive. All three plots are normalized. The value normalized to is the best intended dose from the original plan. The dosage are normalized in order to compare all fractions from all patients. - Except patient 5 as mentioned above.
As seen in figure: 25 neither the bladder nor the rectum has any chance in dose from the scheduled to the adapted plan or again to the verification. The CTV on the other hand improves a lot, it can be seen that the boxplot is much narrower around the intended dose and it almost keeps the effect after the adaptation phase.

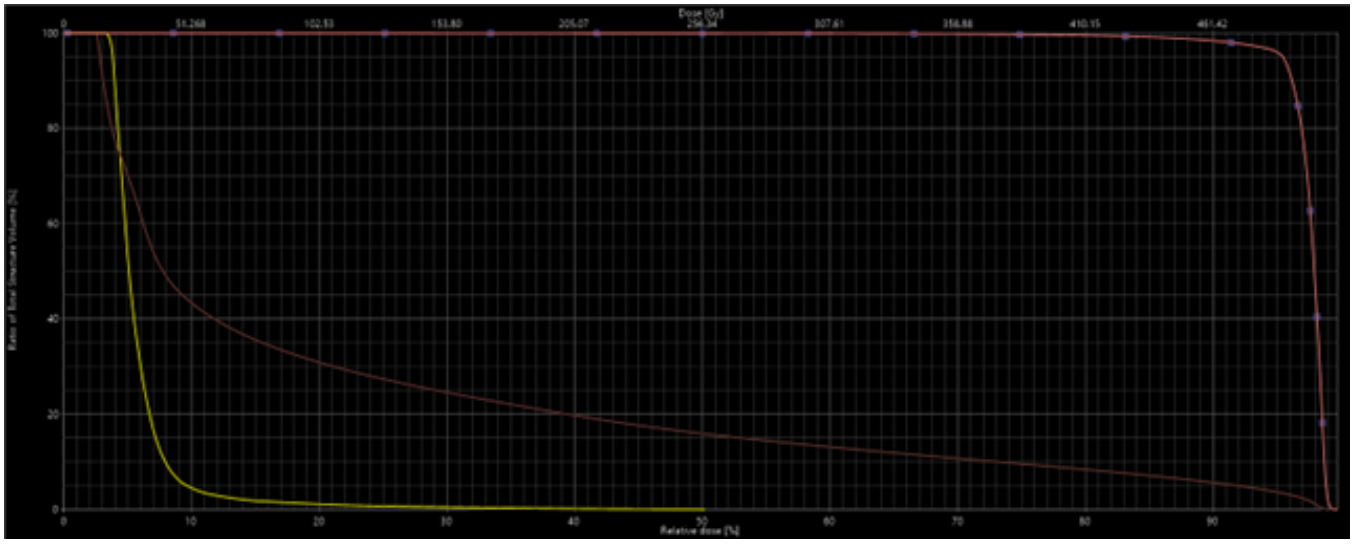

Figure 26: DVH taken directly from Ecplise showing where the data to figure: 25 comes from. - The yellow line being the bladder, the brown the rectum and the red/pink CTV50. [12]

2.4 Discussion

We expected the bladder to be easily drawn by the automated structure drawing tool, but as seen in figure: 24, it does seem like that structure is the structure most often redrawn after the CTV. We had that expectation due to the bladder having a very uniform shape, and also having a good edge contrast to the surrounding tissue.

The adaptive verification plans underwent a complete adaptation process, with the noticeable difference that it was a physicist that drew the anatomical changes and not a doctor. This will introduce some uncertainties in the outcome of the adaptation. But we had the help of physician approved contours from the original plans, significantly lowering the uncertainty.

The delivery / treatment phase takes around 5 minutes, and during this time we could encounter anatomical changes, but it is not feasible to take an additional CBCT after treatment, to make sure this was not the case, because this would increase the dose unnecessary to the patient. But during the 15 minute adaptation phase almost no changes were seen, so it is safe to assume that an additional 5 minutes would not give rise to large anatomical changes.

2.5 Conclusion

Based on the results it is clear to see a significant gain in using adaptive planning to increase CTV coverage. But there is no dosimetric gain observed towards the OARs.
The adaptive workflow is robust across the adaptation phase and is now implemented as the standard treatment offer for patients with vulvar cancer. These conclusions are derived from fraction based data.

3 Chapter 3 - Dose accumulation across all adapted fractions

3.1 Introduction

In chapter 2 we saw that the adaptation worked, when looked at per fraction. In chapter 3, I have used deform image registration as a tool to be able to summarize dose for all adapted fractions per patient. To see if there over all fractions should be a difference in dose to either CTV or OARs.

3.2 Methods

In order to summarize the dose from all factions, we need too use take all doses for a specific patient and summarize them on a common image, in this case I used the original CT scan for the patient. I used that image because it is a ”neutral” image, meaning non of the doses I would like to sum originates from that scan.
The deform image registration needed in order to do this comes in several steps:

As seen in figure: 27, the fixed image and the moving image does not overlap very well, in order to transfer the dose to the fixed image, the moving and the fixed image must completely overlap.

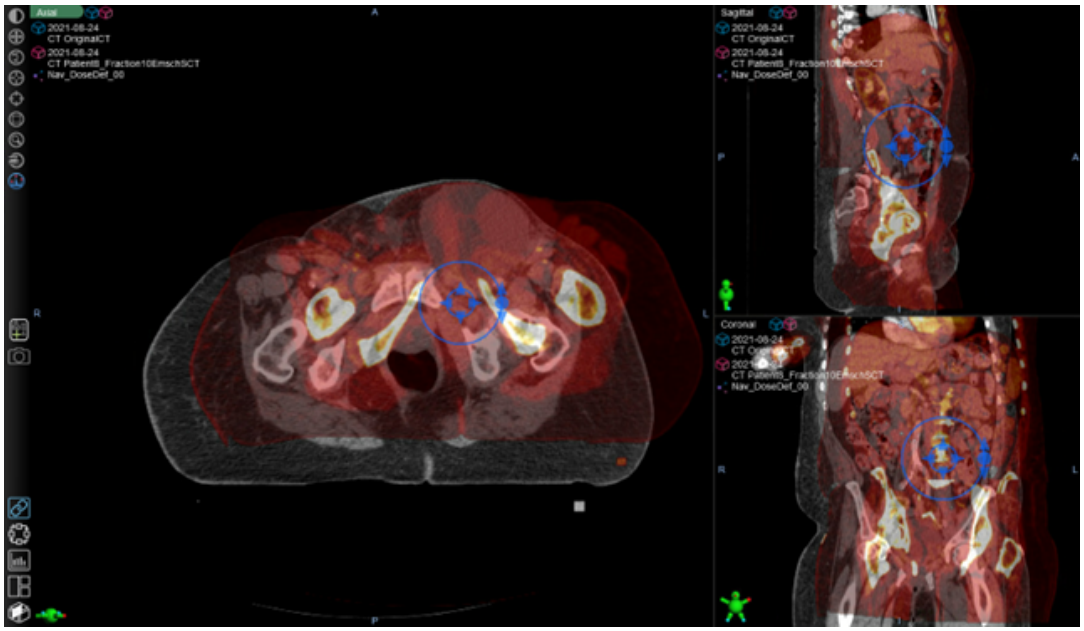

Figure 27: Showing the fixed image (white), and the moving image (red)

Step 1: I had to manually place the moving image on top of the fixed image. In all three dimensions. Figure: 28

Figure 28: Manually overlaid moving and fixed image.

Step 2:
Choose the region of interest, ROI. The ROI should include all parts that receive any dose. Figure: 29

Figure 29: The ROI is manually marked with a red box

Step 3:
Run a rigid deformation. Based on the ROI, the computer automatically adjusts my manual placement. At this step, no changes are made to the moving image, it is only moved as a whole. In this case the rigid deformation did nothing, as my manual placement was as good as could be. But the two images does not overlap completely yet.

Step 4:
Now run the deform image registration. As seen in figure: 30. The two images now completely overlap.

Figure 30

When the two images now overlap it is possible to move the dose matrix from the moving image to the fixed.

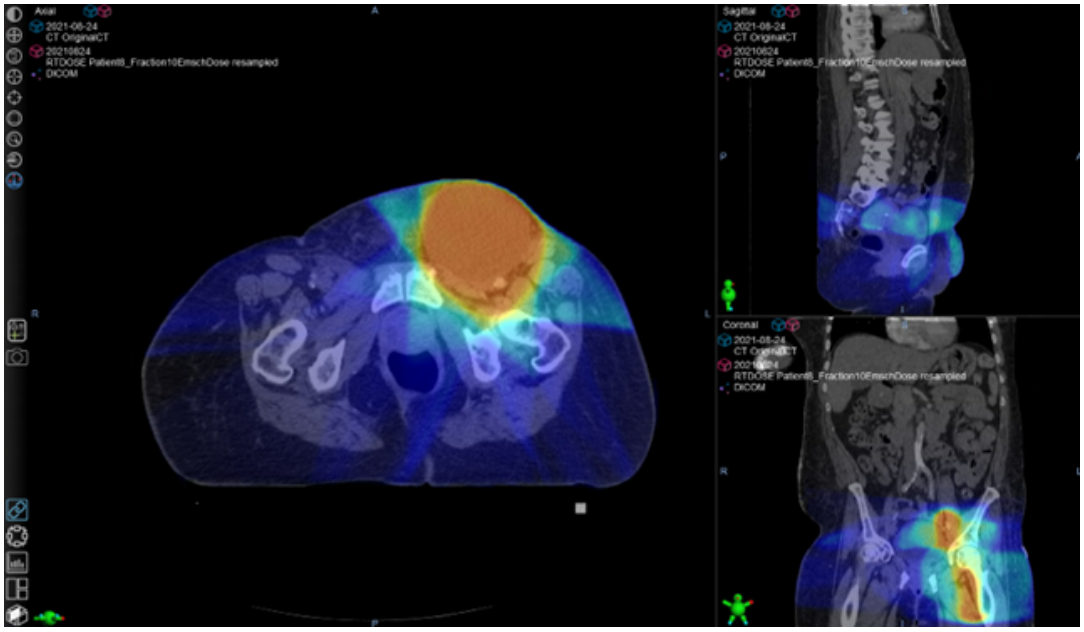

Figure 31

When this is done for all fractions, it can be summarized. The deform image registration is needed because without it the dose matrices would not match in size and therefore I would not

be able to summarize them.

3.3 Results

Again Patient 5, is not part of the data, due to the emulator not being able to make a plan with the extended CBCT. All 9 other patients fractions have been summarized, and the DVH are presented below.

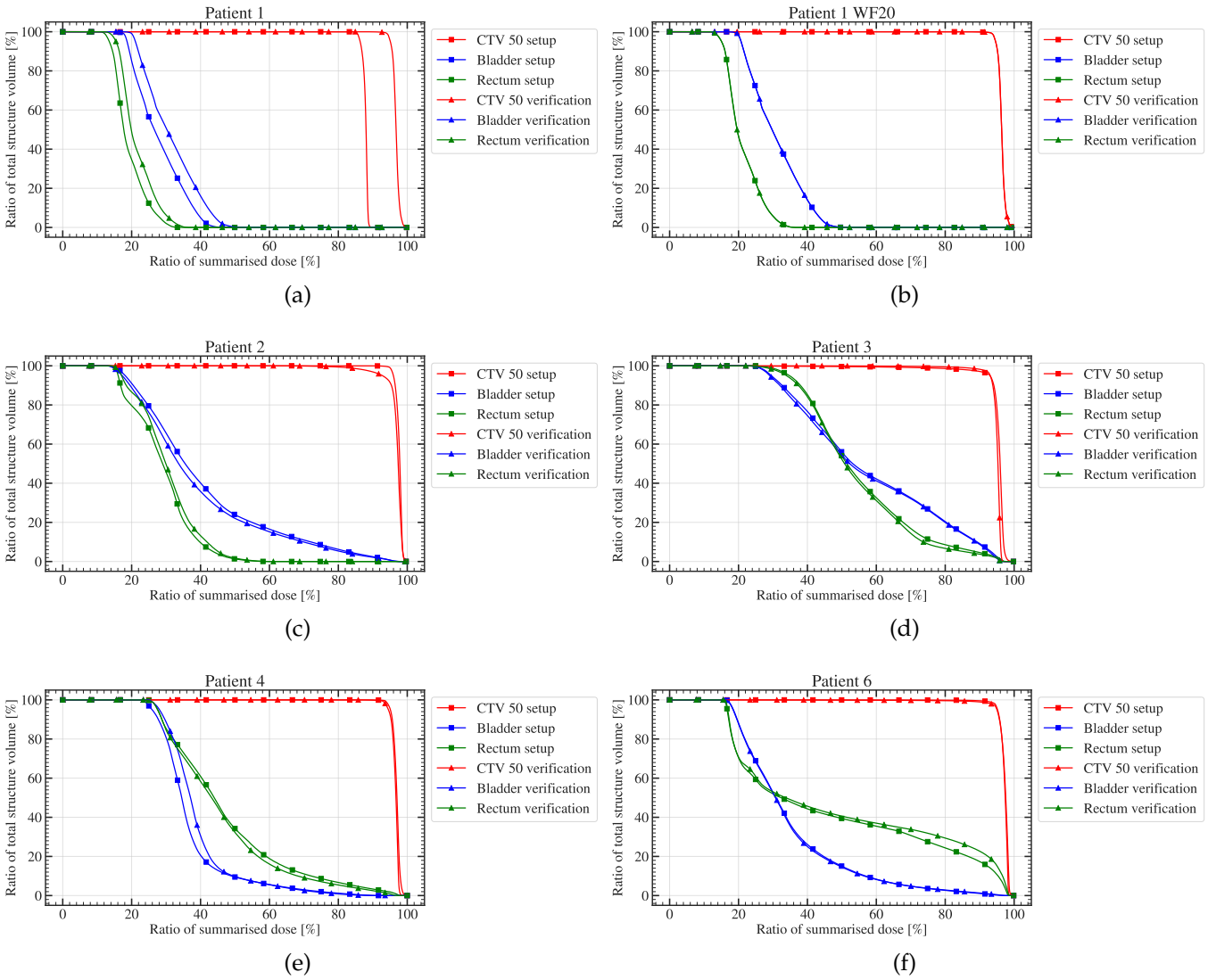

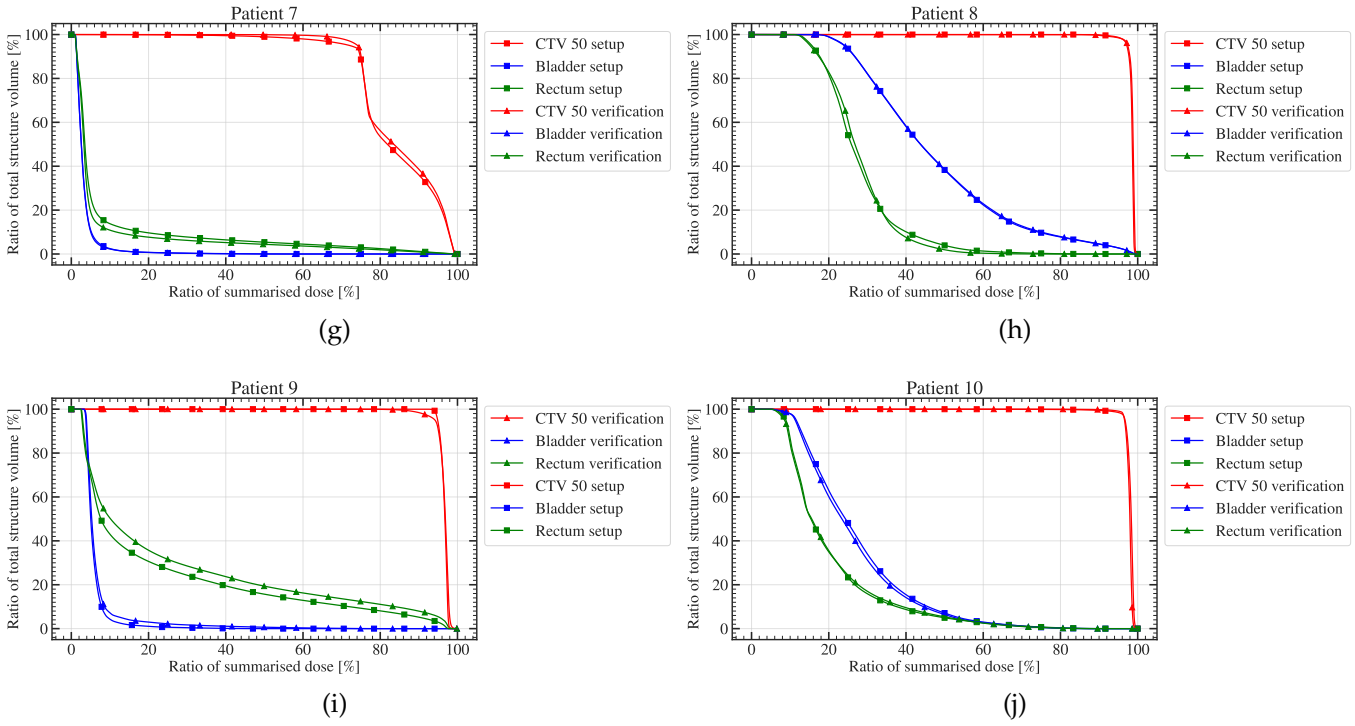

Figure 31: All 10 DVH are plotted similarly. In Patient 9 the legend is reversed compared to all other DVH, this has nothing to do with the plot itself, it was a data import to Python that flipped it.
On the x-axis we have ratio of summarized dose [%], the data is normalized to percent so it can be compared to all other DVH. On the y-axis we have the ratio of total structure volume [%].
All 10 DVH are also in appendix B, in a larger format.

Patient 1: The lines for CTV50 should more or less follow each other as it does in all other DVH. But it does not. The problem is in fraction 20, so I removed it, and generated a DVH without fraction 20 - Patient 1 WF20. In that case both profiles lies exactly on top of each other. After some work we could not find out what coursed the DVH of patient 1, to behave differently than all other DVH.
Generally speaking the dose to CTV 50 is a bit lower on the verification plans, and the dose to OARs are a bit higher.
For patient 7 the CTV50 is cutting of way before the rest. It is because patient 7 also has a CTV65 that is not plotted.
Of the 27 total fraction of each patient, only fractions where the adapted plan was used clinically is summarized here.

3.4 Discussion

For patient 1 the reason for the DVH problem could be that the Patient had the first 20 fractions on a regular plan, and then converted to the adaption. This could give some import problems in the emulator, that was our best bet.
A disadvantage of doing the summarizing in this manner is that the verification plan, is still

build on my own adaptive flow, and has not been cleared by a doctor. So the uncertainty from chapter 2 is carried over in to chapter 3.

3.5 Conclusion

We can again see, that even over all fractions there is no clinically significant loss of plan quality over the course of the adaptation phase. The 15 minutes does not prove to change the outcome of the dose delivered.
That means that we also can conclude for this test, that the robustness of the plan can withstand the 15 minutes the adaptation phase takes.

4 Conclusion

Based on the conclusion from both chapter 2 and 3. It has been shown that both if examined fraction by fraction or summarized over all fractions. That the robustness of the plan over the adaption phase holds. It has also been shown that the CTV has a better coverage with a smaller uncertainty, when using the adaptive plans compared to the scheduled plan.

Further work could be to examine if it is possible to decrease the PTV margin from 5mm to 3 or even 2mm and still have the same coverage of the CTV but also decrease the dose delivered to the OARs.

Acknowledgements

References

[1] Anders Brahme. "Development of Radiation Therapy Optimization". In: Acta oncologica 39 (Feb. 2000), pp. 579–95. DOI: 10.1080/028418600750013267.

[2] M.O. Akpochafor et al. "Simulation of the Linear Boltzmann Transport Equation in Modelling Of Photon Beam Data". In: IOSR Journal of Applied Physics 5 (Nov. 2013). DOI: 10.9790/4861-0567286.

[3] Eclipse Photon and Electron Reference Guide - Version 15.5. Oct. 2017.

[4] Annemari Groenewald. "Design of a universal phantom for quality assurance in diagnostic radiology x-ray imaging". PhD thesis. Aug. 2017. DOI: 10.13140/RG.2.2.13548.00645.

[5] Bruce Hasegawa Jack Lancaster. Fundamental Mathematics and Physics of Medical Imaging. 1st ed. Series in Medical Physics and Biomedical Engineering. CRC Press, Taylor Francis Group, 2017. ISBN: 9781498751612.

[6] Siyong Oh Seungjong ;Kim. "Deformable image registration in radiation therapy". In: Radiation Oncology Journal 2017-jun 30 vol. 35 iss. 2 35 (2 June 2017). DOI: 10.3857/roj.2017.00325. URL: libgen.li/file.php?md5=d2f3b8d9de800977d0905adb5683af3d.

[7] Francis Fortin. Hounsfield Scale (diagram): Radiology case. May 2020. URL: https://radiopaedia.org/cases/hounsfield-scale-diagram.

[8] Tessa Sawyers. CT scans vs. mris: Differences, benefits, and risks. Aug. 2020. URL: www.healthline.com/health/ct-scan-vs-mri#ct-scan.

[9] Sarah Abdulla. Acquiring an image part 1. Oct. 2021. URL: https://www.radiologycafe.com/frcr-physics-notes/ct-imaging/acquiring-an-image-part-1/.

[10] Filtered backprojection (FBP) illustrated guide for Radiologic Technologists. Apr. 2022. URL: https://howradiologyworks.com/filtered-backprojection-fbp-illustrated-guide-for-radiologic-technologists/#what-is-a-ramp-filter.

[11] Andreas Maier. The Math Behind Computed Tomography. Mar. 2022. URL: https://akmaier.medium.com/the-math-behind-computed-tomography-34b8008626df.

[12] Malene E. Bak; et. al. "Clinical experiences with online adaptive radiotherapy of vulvar carcinoma". In: Undergoing revision after first rejection from journal (). Can be found in Appendix A.

[13] X-ray image formation and contrast - sprawls. URL: http://www.sprawls.org/resources/CTIMG/module.htm.

Appendices

A Clinical experiences with online adaptive radiotherapy of vulvar carcinoma

[Page intentionally left blank]

Clinical experiences with online adaptive radiotherapy of vulvar carcinoma

Malene E. Bak*, Nikolaj K.G. Jensen*, Trine J. Nøttrup*, Hanne F. Mathiesen*, Jonathan P.F. Gammeltoft**, Henrik Roed*, Maria Emma Eva Sjölin*, Flemming Kjær-Kristoffersen*, Ivan R. Vogelius*

*Rigshospitalet, Department of oncology, Copenhagen, Denmark

**Faculty of Science, University of Copenhagen, Denmark

Abstract

Background and purpose: Postoperative radiotherapy for vulvar carcinoma is challenging due to a high burden of radiation sequelae, relatively high risk of locoregional disease recurrence, technically challenging target, and postoperative lymphocele. We aim to demonstrate that online adaptive radiotherapy can be used to account for interfractional anatomical changes observed in this patient group.

Materials and methods: 10 patients with vulvar carcinoma (252 fractions) were treated adaptively on an Ethos accelerator. Setup CBCTs were acquired daily for adaptive planning. Verification CBCTs were acquired immediately prior to dose delivery. CTV dose coverage and dose to bladder and rectum were extracted from the scheduled and adapted plans as well as from adapted plans recalculated based on verification CBCTs. In addition, analysis of the decision of the adaptive procedure was performed for 7 patients (170 fractions).

Results: Mean CTV D95% was 97 ± 8% for the scheduled plan compared to 100.0 ± 0.3% and 100.0 ± 0.6% for the adapted plan on the setup and verification CBCT respectively. Dose to OARs varied substantially and did not show any benefit from adaption. The adapted plan was chosen for 60% of the fractions and dominant reasons for not adapting were “no significant dosimetric gain” (29 fractions) and “MD not available for treatment” (19 fractions). The adaption time was 15 min on average.

Conclusion: CTV dose coverage was significantly improved with adaptation compared to image-guided RT. This gain was robust during the time on the couch. No significant dosimetric gain was observed for normal tissue.

Keywords

Online Adaptive Radiotherapy, deformable image registration, vulvar neoplasms, computer assisted radiotherapy planning, workflow.

Highlights

- Online ART makes it possible to obtain better target coverage for patients with vulvar carcinoma.
- The adaptive workflow is robust to the longer treatment time and smaller anatomical changes during that time.
- ART for gynecological cancers does not reduce normal tissue dose without margin changes.

Introduction

Vulvar carcinoma is a rare malignancy that accounts for 0.3% of all cancers globally, with an incidence of approximately 45,000 new cases and 17,000 deaths per year (2020)[1]. From 1978 to 2006, an increase of 1.6% per year has been observed for women under 60 years in Denmark, while the incidence has remained unchanged for women over 60[2].

Current treatment involves surgical resection of the primary vulvar lesion. Inguinal lymph node dissection (or sentinel lymph node staging) is performed if the primary tissue invasion exceeds 1 mm or clinically and/or radiographically suspected nodes. If lymph nodes are positive, current guidelines advise full inguinal lymph node dissection and adjuvant external beam radiation therapy (EBRT) with or without chemotherapy for macrometastases and adjuvant external beam radiation therapy (EBRT) with or without chemotherapy for micrometastases[3][4].

Radiotherapy has a major role in curative treatment of vulvar carcinoma patients. Postoperative radiotherapy for vulvar carcinoma is challenging due to a high burden of radiation sequelae, relatively high risk of locoregional disease recurrence and technically challenging targets combined with common postoperative lymphocele causing anatomical variations on a daily basis. These factors are traditionally accounted for by a safety margin around the clinical target volume (CTV) to yield a planning target volume (PTV) to be irradiated encompassing the predicted deviations and ensure target coverage[5]. This, however, causes the treatment field to include more healthy tissue in the high dose area which increases the risk of side effects. Adaptive radiation therapy (ART) can be used to reduce the safety margin and still account for both systematic and random complex anatomical changes as well as time trends[6]. In ART with daily online (real-time) replanning, the dose plan is reoptimized based on the anatomy of the day in every treatment fraction[7].

Standard EBRT radiation treatment takes approximately 20 minutes per fraction at our center. It's critical that the online ART implementation does not add considerably to this, as prolonged treatments increase the risk of intrafractional variations and can be difficult for the patient to endure[8]. In addition, the monetary cost of providing care would increase if ART requires substantially longer timeslots.

All the above considerations made postoperative vulvar carcinoma patients a preferred group for early experiences with online adaptive radiotherapy on a dedicated Ethos accelerator[9].

The aim of this study is to test whether online ART is relevant for these patients and if it improves target coverage and/or reduces dose to organs at risk (OAR). We also aim to analyze the adaptive workflow with respect to treatment time and the workload of manual editing.

Materials and methods

Ethos planning system

All patients were treated on a Varian Ethos accelerator (Varian Medical Systems, Palo Alto, CA) and were simulated in a Siemens CT scanner. Planning CT-scans were acquired with and without intra-venous contrast (Optiray 300). This ensured optimal conditions for the oncologist to contour relevant structures while having non-contrast planning scans for dose calculation and adaption to the non-contrast CBCT scans at each treatment fraction.

Treatment plans were generated semi-automatically by choosing several dosimetric goals for the target and OAR. At the baseline CT scan, we requested the creation of a 7, -9, and 12 equidistant IMRT fields plans for adaption and plans with 2 and 3 full VMAT arcs for comparison. The VMAT plans were not used for adaption, as the calculation time during the adaptive flow is prohibitive. The best IMRT plan, based on 12 preset dose constraints and target coverage for planning, was chosen as the reference plan for adaptation. The specific beam geometry (number of beams, collimator, and gantry angle) from the reference plan was used for every adapted fraction.

The daily adaptive procedure started with conventional patient positioning and a CBCT scan. Target and normal structures were transferred from the planning CT simulation to the CBCT scan of the day using a proprietary algorithm[10]. The algorithm relied on a hybrid matching of intensity and predefined "influencer structures". Influencer structures must be reviewed and when necessary corrected manually before the remaining structures were propagated.

In this study, influencer structures were chosen to be bowel, rectum, and bladder for the first two patients but was changed to rectum and bladder for the subsequent patients due to excessive time needed to correct the automatic delineation of the bowel. Targets and the remaining OAR structures were then deformed by the same hybrid AI algorithm as the influencer structures, accounting for the approved influencer structures. These structures were reviewed and approved by a specialist gynecological radiation oncologist, after editing as needed.

An adapted plan was created by reoptimizing the reference plan to the daily anatomy. The system calculated the dose distribution of the reference plan "scheduled plan" for comparison (a deformable image registration (DIR) of the baseline CT Hounsfield unit map to the CBCT was used as the electron density of the day[10]). The physician and physicist decided which plan to treat ("scheduled" or "adaptive") and approved it for treatment. In the absence of a specialist oncologist on the day, only the scheduled plan was allowed for treatment.

A verification CBCT was acquired just before treatment delivery to ensure no clinically relevant changes in positioning or anatomy of the patient had occurred during adaption. The couch position could be corrected if needed. The chosen plan was validated through a QA process using Mobius3D (Varian Medical Systems, Palo Alto, CA), which include an independent MU dose calculation prior to treatment (the adaptive workflow is depicted schematically in Figure 1).

Offline simulation of robustness of the adapted plans

We performed a validation of the quality/robustness of the adaptive plans with regards to the uncertainties arising from motion during the adaptation workflow by recalculating the dose distribution from the adapted plan on the verification CBCT. This procedure was implemented to ensure the treatment was as secure as a traditional image-guided radiotherapy (IGRT). A post-treatment CBCT was not acquired due to imaging dose concerns (CTDI dose is 41.9 mSv). Plan recalculation on the verification CBCT was performed

on a stand-alone Ethos emulator and required substantial manual import/export maneuvers. The dose covering the hottest 2% of the bladder and rectum, and the minimum dose covering 95% of the CTV dose (D95%) were extracted from scheduled, adapted and verification plans.

Patients

Daily adaptive radiotherapy became available in our department on January 22, 2021 and vulvar carcinoma were prioritized for the adaptive treatment slots as part of routine clinical treatment decision. After a short run-in period, the daily adaptive workflow became the standard treatment offering for vulvar carcinoma patients at our institution. Here, we report on the first 10 vulvar carcinoma patients referred for radiotherapy with daily adaptation on the Ethos accelerator. Patient characteristics are described in Table 1. Patient 1 was an ongoing patient in the clinic who only got the last 8 fractions of the treatment on the adaptive workflow. Collection and reporting of the data were performed with authorization from departmental review and regulatory approval as quality assurance of the clinical procedures.

Patient number	Age	Primary disease/recurrence	FIGO stage	No. of lymph node metastases	Operation T site*	Radiation field including vulva	Radiation field including uni- or bilateral groin
1	85	Primary	IIIA1	1	R0	No	Yes, unilateral
2	83	Primary	IIIA	2	R0	No	Yes, unilateral
3	80	Primary	IVB	22	R1	Yes	Yes, unilateral
4	63	Primary	IIIA (ii)	1	R0	No	Yes, bilateral
5	84	Recurrence	IIIB	1	R1	Yes	No
6	71	Recurrence	IB	1	R0	Yes	Yes, unilateral
7	43	Fourth recurrence	-	-	Inoperable	Yes	No
8	59	Primary	IIIA	1	R0	No	Yes, unilateral
9	54	Primary	IB	-	R1	Yes	No
10	46	Primary	IB	1	R1	Yes	Yes, unilateral

Table 1. Patient demographics. **R0 = Free margin, R1= Not sufficient margin*

Patients 1-3 were planned with an isotropic PTV margin of 7 mm from CTV, which is standard for non-adaptive treatments in our clinic. CTVs were delineated by the oncologist based on CT images. Starting with patient 4 PTV margins were reduced to 5 mm.

Figure 1 shows how the dosimetric data was collected. Data includes all fractions where the physician approved the adapted structures, the treating physician did occasionally select the scheduled plan without finalizing contouring for adaptive workflow with reasons provided in the questionnaires. 34 adapted

fractions were not recalculated due to import problems in the emulator. This problem was random for all patients except patient 5 where the emulator couldn't handle extended CBCT scans.

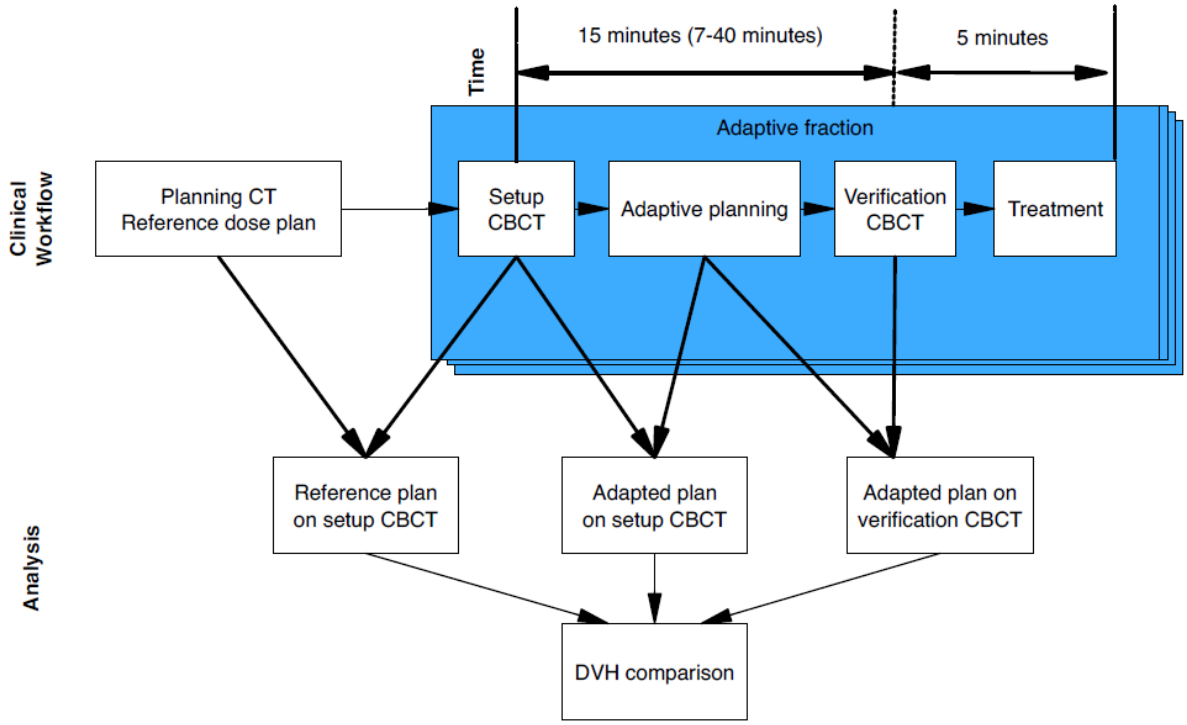

Figure 1 – Adaptive treatment and subsequent data collection workflow

Starting with patient 4, we implemented a daily questionnaire including details on the quality of the automatic contouring of OARs and target, how many CBCT slices that needed to be contoured/edited as well as the reason for the choice of plan of the particular day. Number of slices that needed editing were counted. Edits were stratified using the definition from Sibolt et al[11]. The reasons for not choosing the daily adaptive plan were categorized as 1) No physician available, 2) No dosimetric gain (between scheduled and adaptive plan), 3) Automatic contouring of either CTV or OARs were too poor, 4) Other and 5) Unknown. Adaption time was recorded from the first CBCT scan to the second verification CBCT scan. This interval includes evaluation and re-contour of target and OAR structures, dose-calculation of scheduled and adaptive plan, plan choice and approval and QA process.

All statistics were performed in R using Wilcoxon paired test or Spearman correlation. The null hypothesis was that there was no difference between the scheduled and adaptive plans, with a significance set at p=0.05.

Results

Dose coverage of the CTV measured by the mean D95% was 97 ± 8% (standard deviation) for the scheduled plan and 100.0 ± 0.3% and 100.0 ± 0.6% for the adapted plan on the setup and verification CBCT respectively. This shows a significant improvement of target coverage with the adapted plan (signrank $p<0.0001$) which was retained at the verification step (signrank $p<0.0001$). The dose received by to the 2% hottest volume of bladder was significantly increased from 86 ± 33% on the scheduled plan to 91 ± 40% (signrank $p=0.0008$), this increase was retained at verification with mean 116 ± 63% (signrank $p<0.0001$). The large standard deviation observed were caused by three patients having very low doses to bladder and three other patients having a small volume of target overlapping the bladder resulting in interfractional variation of bladder dose, which were amplified by normalization. Rectum dose was unchanged by adaptation with mean 101 ± 35% on the scheduled plan and 102 ± 23% on the adapted plan (signrank $p=0.09$), however at verification it was significantly higher than scheduled plan with mean 108 ± 31% (signrank $p=0.004$), cf. Figure 2. All treated plans met the predefined dose constraints. See appendix for supplementary figures.

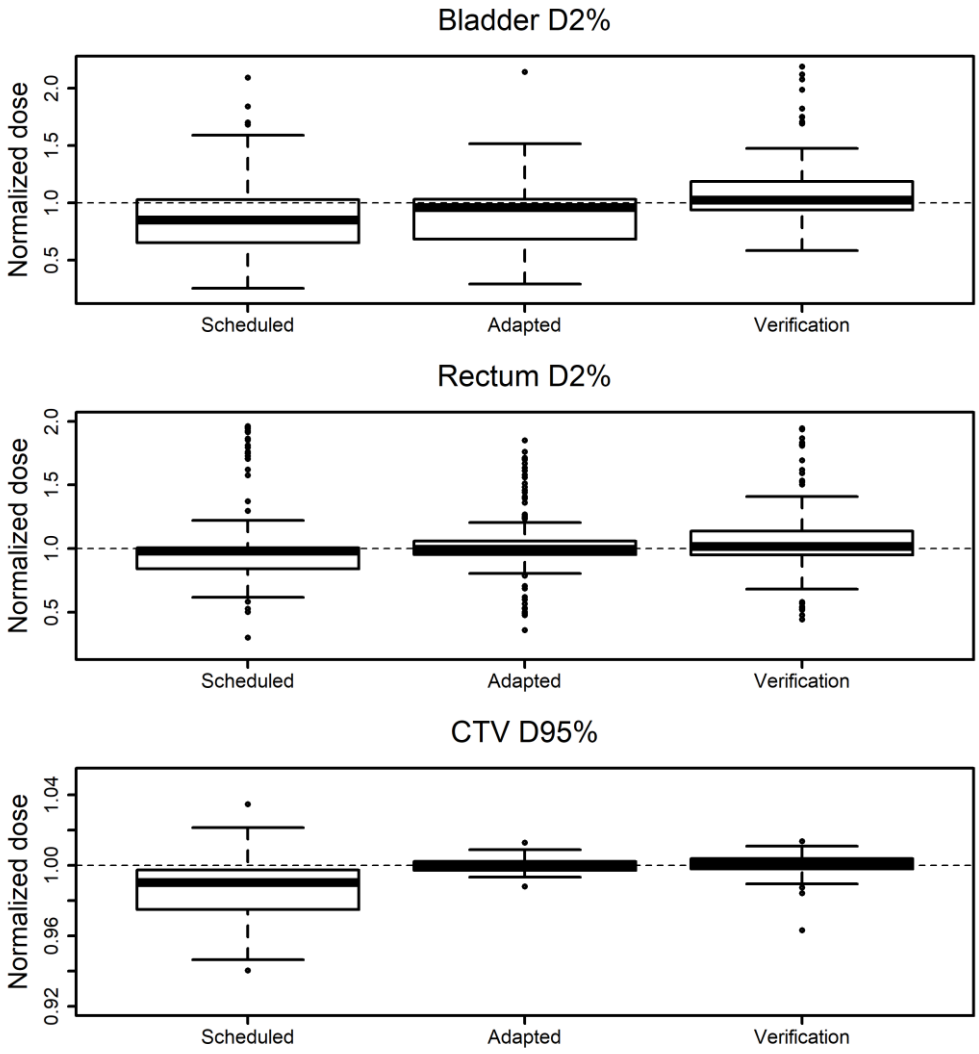

Figure 2 – Normalized dose to reference plan for scheduled plans, adapted plans and verification plans for bladder (D2%), rectum (D2%) and CTV (D95%) respectively for patients 1-10. Dashed lines indicate reference dose. The figure excludes 3 upper outliers on bladder adapted, 2 upper outliers on bladder verification and 5 lower outliers on CTV scheduled to improve visualization.

The number of slices where OAR and target structures that were edited varied substantially between patients, cf. Figure 3. For bladder no edits were required for 43% of fractions, minor edits for 8% of fractions and moderate/major edits 49% of fractions. Rectum needed no edits 66% of fractions, minor edits 9% of fractions and moderate/major edits 25% of fractions. Lastly, CTV needed no edits 48% of fractions, minor edits 17% of fractions and moderate/major edits 35% of fractions.

For bladder, patients 5, 6 and 7 only needed minor recontouring with a mean change of <2% of the slices while patient 4, 8, 9 and 10 had larger need for recontouring with a mean change of >35%. For rectum we observed a general good delineation by the system with a mean change of <12%. We observed <3% edits for all patients except patient 8. The number of slices with edits needed for CTV varied a lot between the patients with a mean of 15% (with range: 0.4%-38%). In general, number of slices with edits of the machine-generated contours did not show any clear association with the proportion of fractions adapted, cf. Figure 4.

Median adaption time was 15 minutes and 75th percentile was 17 minutes, cf. Figure 3. A correlation coefficient of 0.47 between adaption time and number of edits suggests only weak correlation, however some increasing trend was observed.

The adaptive plan was chosen for 150 out of 252 fractions (60%). The proportions of adapted vs. scheduled plans and the aggregated distributions of the reasons not to adapt are shown in Figure 4. Dominant reasons for not adapting were “no significant dosimetric gain” (29 fractions) and “MD not available for treatment” (19 fractions).

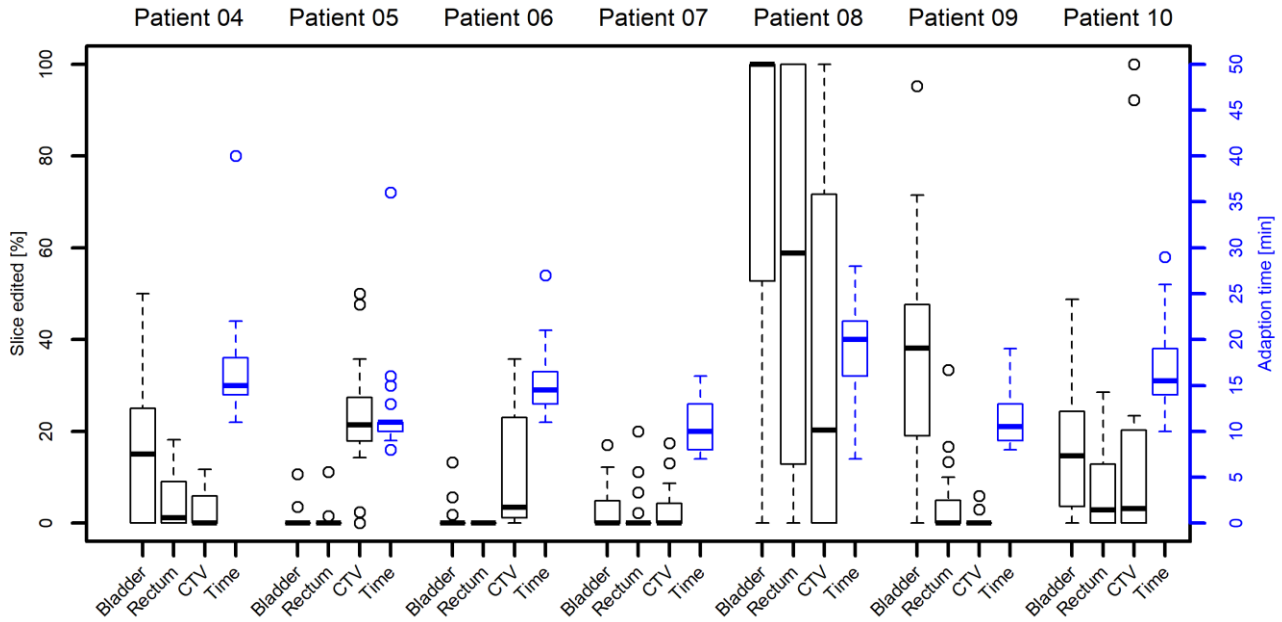

Figure 3 – Proportion [%] of recontoured slices of bladder, rectum, and CTV for patient 4-10 as well as the adaption time.

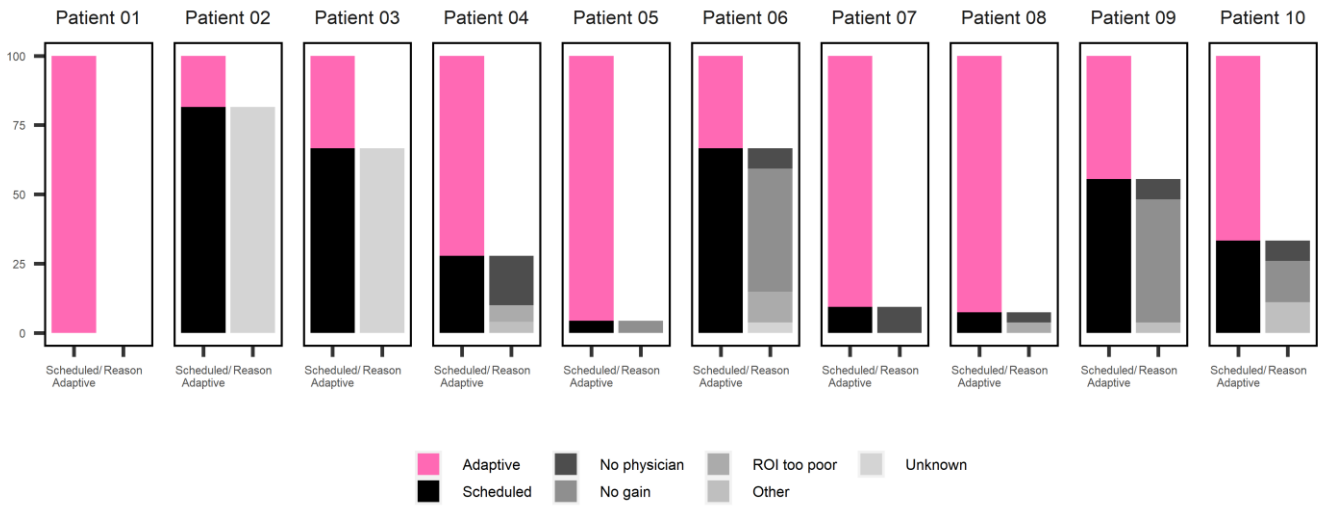

Figure 4 - Distribution of chosen adapted vs scheduled plan for patient 1-10. Reasons for not choosing an adaptive plan is also shown for each patient. Patient 1 was the pilot patient and was only treated with the adaptive workflow for the last 8 fractions. Patient 1-3 wasn’t included in the daily registration and reasons are therefore unknown.

Discussion

There was a significant advantage in CTV coverage using an adaptive workflow compared to IGRT in this study. The adaptive plans were shown to be robust to anatomical change during the adaption process. A limitation of this comparison is that we did not perform a post-treatment CBCT but analyzed stability on the verification CBCT prior to dose delivery. This choice was made as the additional imaging dose could not be justified in this routine treatment setting. However, it is considered unlikely that substantial changes would occur during the approximately 5 minutes delivery time when the dosimetric impact of anatomical changes occurring during adaption time (15 minutes) was as limited as observed in Figure 1. We therefore conclude that for vulvar carcinoma patients the comparison of scheduled and adapted plan on the setup CBCT is a reliable representation of the delivered dose.

The adaptive plans were recalculated using the emulator and the simulation requires manual recontouring of OARs and CTV which introduces some uncertainties. A physician was not present at this time-consuming procedure and it is acknowledged that this may impact the results. The involved physicist had access to physician approved contours which was used to produce an acceptable estimate.

The observed improvement in target coverage with adaptation indicates that even with a smaller PTV margin of 5 mm, the plans were still able to meet the clinical goals. No direct benefit for dose to bladder and rectum was demonstrated. It may be possible to reduce margins even more as adaptation eliminates the need to account for interfractional uncertainties, such a margin reduction would be expected to reduce OAR doses. Margin reduction should be investigated further but a “fall back” option of conventional margins may be necessary as our results indicate that it is unlikely that every fraction can be adapted.

Mean total treatment time, including patient positioning, image acquisition, adaption, and beam-on time was estimated 45 minutes, as time to position patient was not recorded. Compared with the normal treatment time of 20 minutes, the adaptive workflow is manageable. We observed some outliers where the adaption time was up to 40 minutes which made the total treatment time up to an hour. Comparing with the ART prostate study by Byrne et al[12] we observe more need for edits as they showed no and minor edits were 11% and 81% of fractions to OARs (rectum, bladder, prostate and seminal vesicle) respectively and no or minor change to CTV was 91%. The ART prostate study by Sibolt et al[11] also reported less need for change of OARs and CTV. An explanation for this difference is that we had different acceptance criteria for the vulvar carcinoma patients. Furthermore, five of the patients in this study received weekly cisplatin and antiemetic drugs which might have led to more gas and faeces in bowel and rectum due to the impact on the gastrointestinal system of these drugs, neither of the patient groups in the Byrne or Sibolt cohorts receive concomitant chemotherapy. Appearance or changes to volumes of air, IV contrast agent or medical devices such as urinary catheters were noted to cause difficulties for the DIR, this increases the need for manual editing of structures by the physicians.

The adapted plan was rejected 40% of the time and we observed that certain patients had a low rate of adaptation which most frequent was explained by no relevant dosimetric gain using the adapted plan compared to the scheduled plan. The second most frequent reason for not choosing an adapted plan was that no physicians were available at the accelerator during treatment. In these cases, we cannot be sure whether an adaptive plan or scheduled plan would have been preferred. The need for specialized physicians trained in daily adaption is therefore critical for complex cases, whereas simpler adaptation cases can be performed by RTTs[11]. For seven fractions the automatic contouring was of such poor quality that manual recontouring was considered unfeasible due to expected adaption time and uncertainty exceeding clinical acceptable goals and for this reason the scheduled plan was chosen.

Concluding on the efficiency of daily adaptive radiotherapy for vulvar carcinoma, it should be acknowledged that a formal health economic assessment is well beyond the scope of this paper. However, we believe that with gradual improvements of procedures and efficiency, online adapted treatment of vulvar carcinoma patients may become a viable routine option in a not-too-distant future and can be expected to lead to some dosimetric benefits.

A practical challenge arises if the quality of the CBCT is insufficient for delineation. In this study, seven fractions had to be treated with the scheduled plan because the physician was unable to contour the CTV, even with the assistance of automatic contour propagation on the CBCT. Improvement of the quality of the CBCTs is therefore key to extend the use of ART.

It's acknowledged that the present report is an assessment of dosimetric precision and technical feasibility of online adaptive RT for vulvar carcinoma. We have not attempted to capture clinical outcome as the study would be severely underpowered to provide informative results thereof. The exposure comparison of organs at risk does not indicate any benefit in terms of normal tissue complication probability without a possible conversion of the improved target coverage to decreased margins. Estimation of the clinical benefit of improved target coverage is too uncertain for meaningful modeling exercises.

This is, however, the first study to our knowledge of daily online adaptive radiotherapy for gynecological cancer and provides indication of feasibility and a direction for future studies of optimal use of this emerging technology.

Conclusion

Online ART has become our departmental standard offer for patients with vulvar carcinoma. There is a significant gain to CTV dose coverage compared to IGRT. The adaptive workflow is robust with respect to the longer total treatment time and smaller PTV margin. No significant dosimetric gain is observed for OARs.

Declaration of Competing Interest

Corporate sponsored research. The authors report research and teaching contracts with Varian Medical Systems, ViewRay Inc and Brainlab, to institution.

Acknowledgement

The RTT's: Elin Ravnkilde Heilmann, Chanette Beck Hansen, Jeannett Linde, Anna Green, Sussi Christensen, Tammie Michelle Sandholdt Jensen, Mai Bryrup Lyhne and Lykke Kildegård Johansen at the Ethos accelerator are acknowledged for their important work on the collection of the qualitative questionnaires.

References

[1] The Global Cancer Observatory, “Glocal Cancer Observatory - Vulva fact sheet,” 2020. https://gco.iarc.fr/today/data/factsheets/cancers/21-Vulva-fact-sheet.pdf.

[2] L. Baandrup, A. Varbo, C. Munk, C. Johansen, M. Frisch, and S. K. Kjaer, “In situ and invasive squamous cell carcinoma of the vulva in Denmark 1978-2007-a nationwide population-based study,” 2011, doi: 10.1016/j.ygyno.2011.03.016.

[3] M. H. M. Oonk *et al.*, “European Society of Gynaecological Oncology Guidelines for the Management of Patients With Vulvar Cancer,” 2017, doi: 10.1097/IGC.0000000000000975.

[4] M. H. M. Oonk *et al.*, “Radiotherapy Versus Inguinofemoral Lymphadenectomy as Treatment for Vulvar Cancer Patients With Micrometastases in the Sentinel Node: Results of GROINSS-V II,” *J. Clin. Oncol.*, vol. 39, no. 32, pp. 3623–3632, Nov. 2021, doi: 10.1200/JCO.21.00006.

[5] M. Van Herk, P. Remeijer, C. Rasch, and J. V. Lebesque, “The probability of correct target dosage: dose-population histograms for deriving treatment margins in radiotherapy,” *Int. J. Radiat. Oncol. Biol. Phys.*, vol. 47, no. 4, pp. 1121–1135, Jul. 2000, doi: 10.1016/S0360-3016(00)00518-6.

[6] J.-J. Sonke, M. Aznar, and C. Rasch, “Adaptive Radiotherapy for Anatomical Changes,” *Semin. Radiat. Oncol.*, vol. 29, no. 3, pp. 245–257, 2019, doi: 10.1016/j.semradonc.2019.02.007.

[7] O. L. Green, L. E. Henke, and G. D. Hugo, “Practical Clinical Workflows for Online and Offline Adaptive Radiation Therapy,” *Semin. Radiat. Oncol.*, vol. 29, no. 3, pp. 219–227, 2019, doi: 10.1016/j.semradonc.2019.02.004.

[8] S. Lim-Reinders, B. M. Keller, S. Al-Ward, A. Sahgal, and A. Kim, “Critical Review Online Adaptive Radiation Therapy,” *Int. J. Radiat. Oncol. Biol. Phys.*, vol. 99, no. 4, pp. 994–1103, 2017, doi: 10.1016/j.ijrobp.2017.04.023.

[9] Y. Archambault *et al.*, “MAKING ON-LINE ADAPTIVE RADIOTHERAPY POSSIBLE USING ARTIFICIAL INTELLIGENCE AND MACHINE LEARNING FOR EFFICIENT DAILY RE-PLANNING,” *Med. Phys. Int. J.*, vol. 8, no. 2, 2020.

[10] V. M. Systems, *Ethos Algorithms Reference Guide*. Varian Medical Systems, 2021.

[11] P. Sibolt *et al.*, “Clinical implementation of artificial intelligence-driven cone-beam computed tomography-guided online adaptive radiotherapy in the pelvic region,” *Phys. Imaging Radiat. Oncol.*, vol. 17, p. 1, Apr. 2021, doi: 10.1016/J.PHRO.2020.12.004.

[12] M. Byrne *et al.*, “Varian ethos online adaptive radiotherapy for prostate cancer: Early results of contouring accuracy, treatment plan quality, and treatment time,” *J. Appl. Clin. Med. Phys.*, 2021, doi: 10.1002/ACM2.13479.

Appendix A. Supplementary data

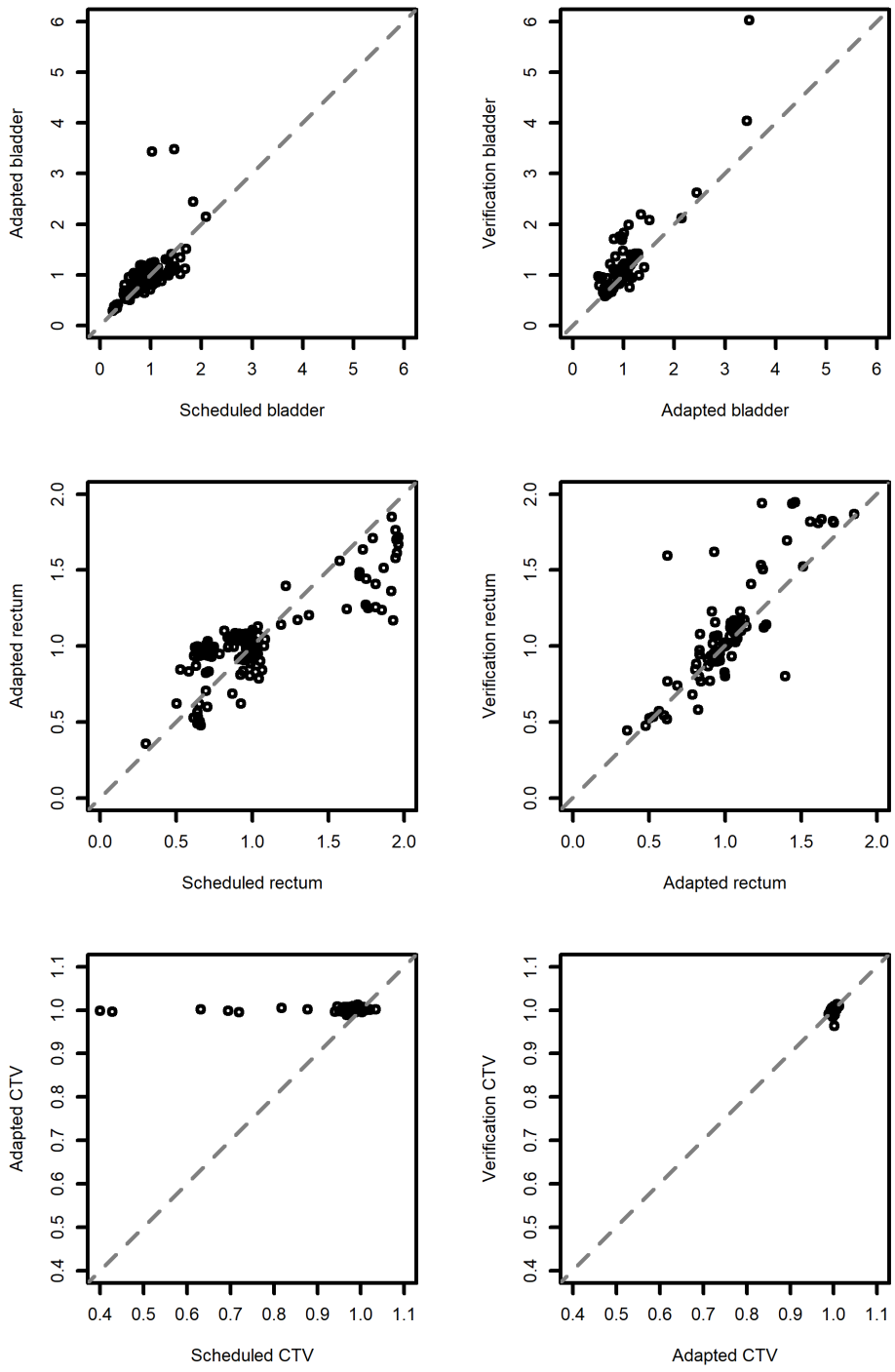

Figure 2 - Scatter plots visualizing normalized doses for scheduled plans versus adaptive plans as well as adaptive plans versus verification plans for OARs and CTV. Upper row shows a positive linear correlation between scheduled and adaptive (ρ=0.82) doses as well as some between adaptive and verification (ρ=0.68) doses. Middle row shows some clustering tendency between scheduled and adaptive (ρ=0.56) doses with higher doses more frequently in scheduled. Between adaptive and verification, we see a positive linear correlation (ρ=0.80). Lower row shows no correlation (ρ=0.23) between scheduled and adaptive doses and it is observed that the adaptive doses doesn't change and are on level with the reference dose. Scheduled doses vary more. A smaller correlation (ρ=0.60) is seen between adaptive and verification doses. The robustness of the adapted plans is clearly visualized.

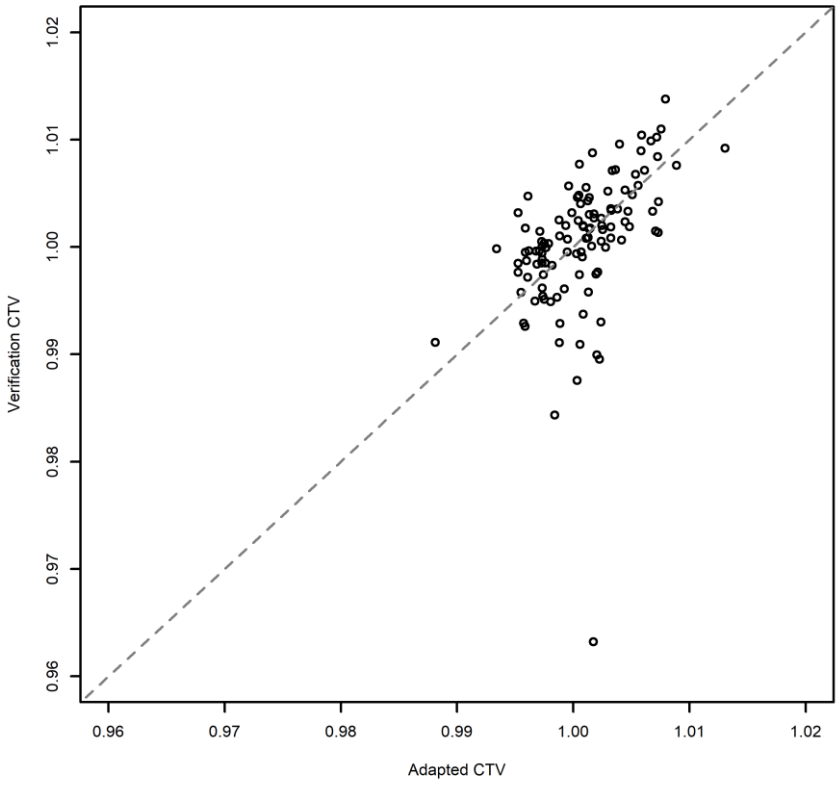

Figure 3 - Scatter plot visualizing normalized doses for adapted plans versus verification plans with narrower axis. Here, the positive linear correlation is more clearly.

B DVH from Chapter 3 - all patients

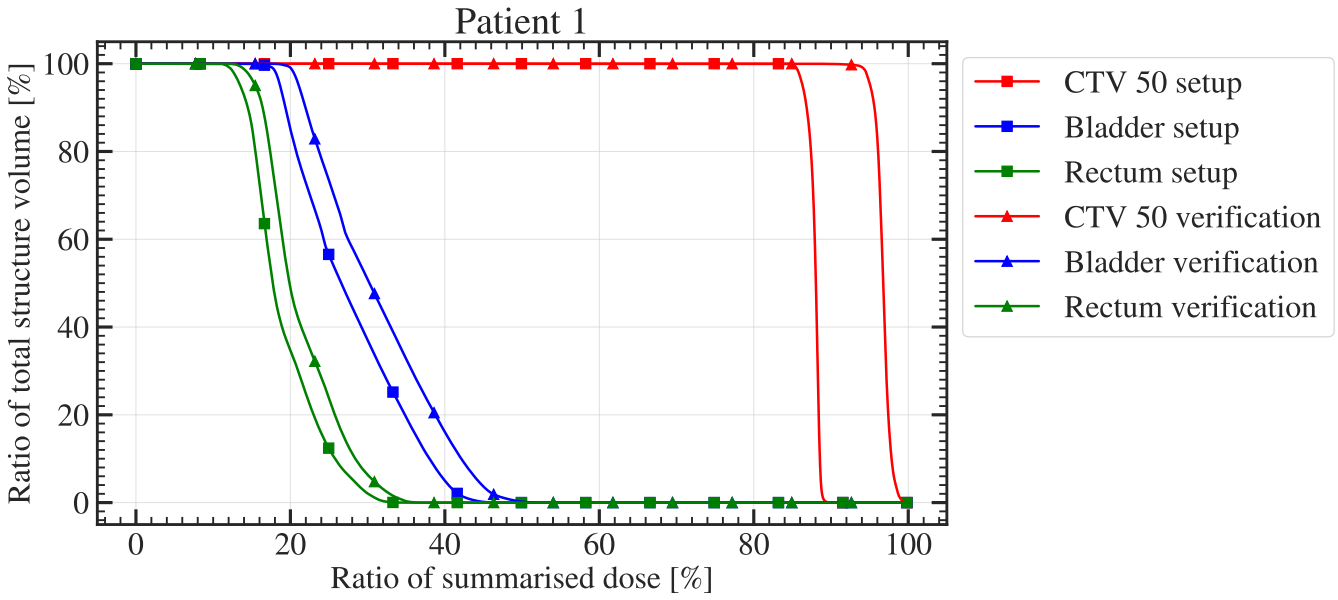

Figure 32

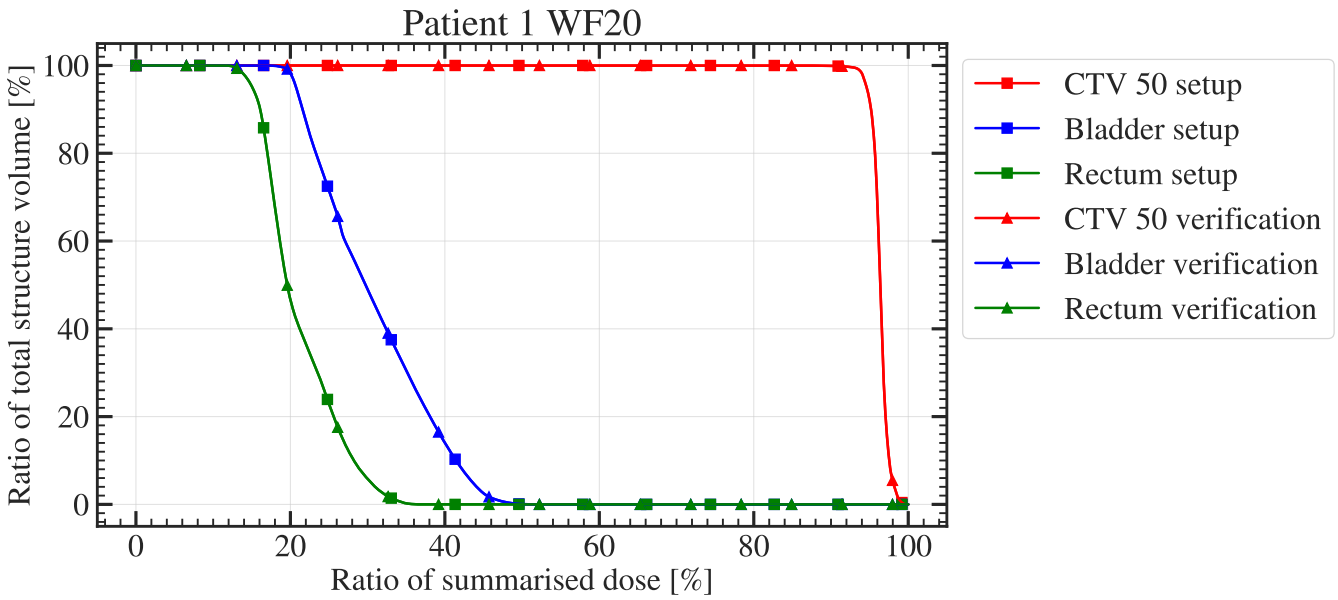

Figure 33

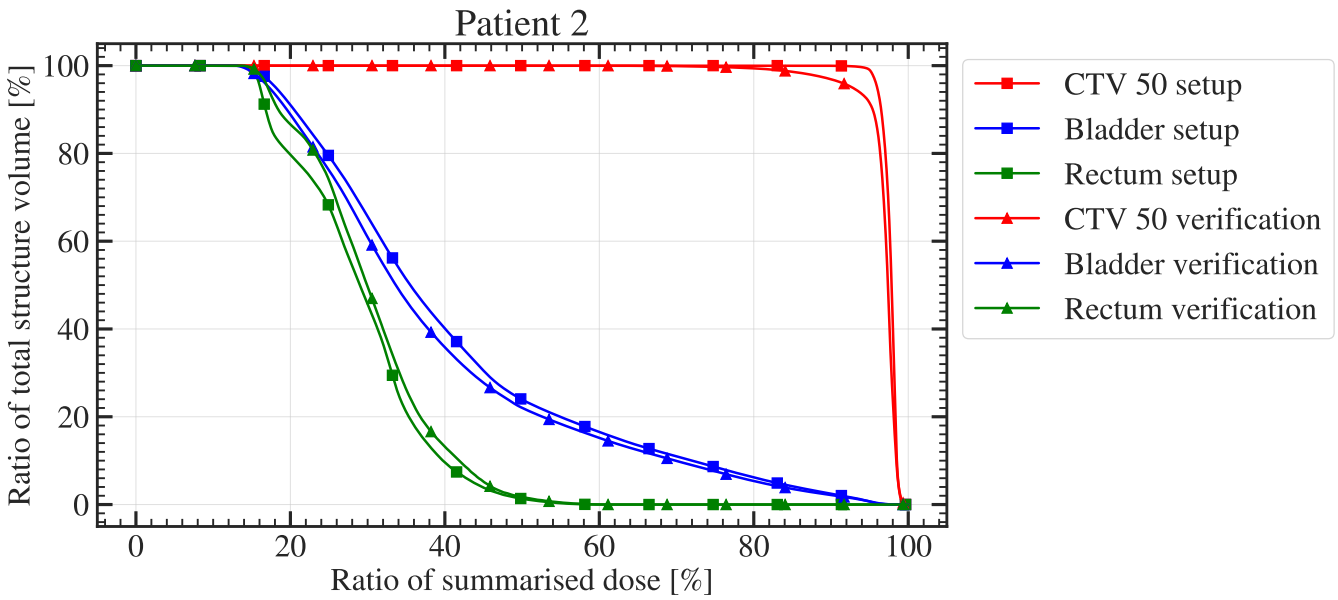

Figure 34

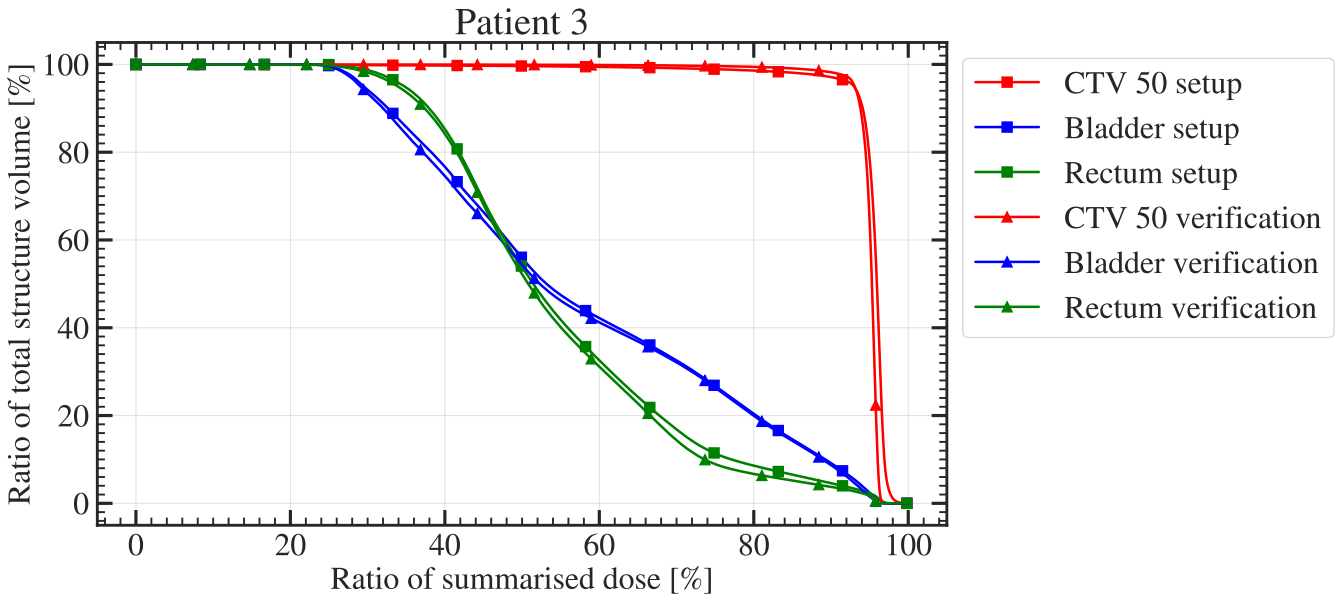

Figure 35

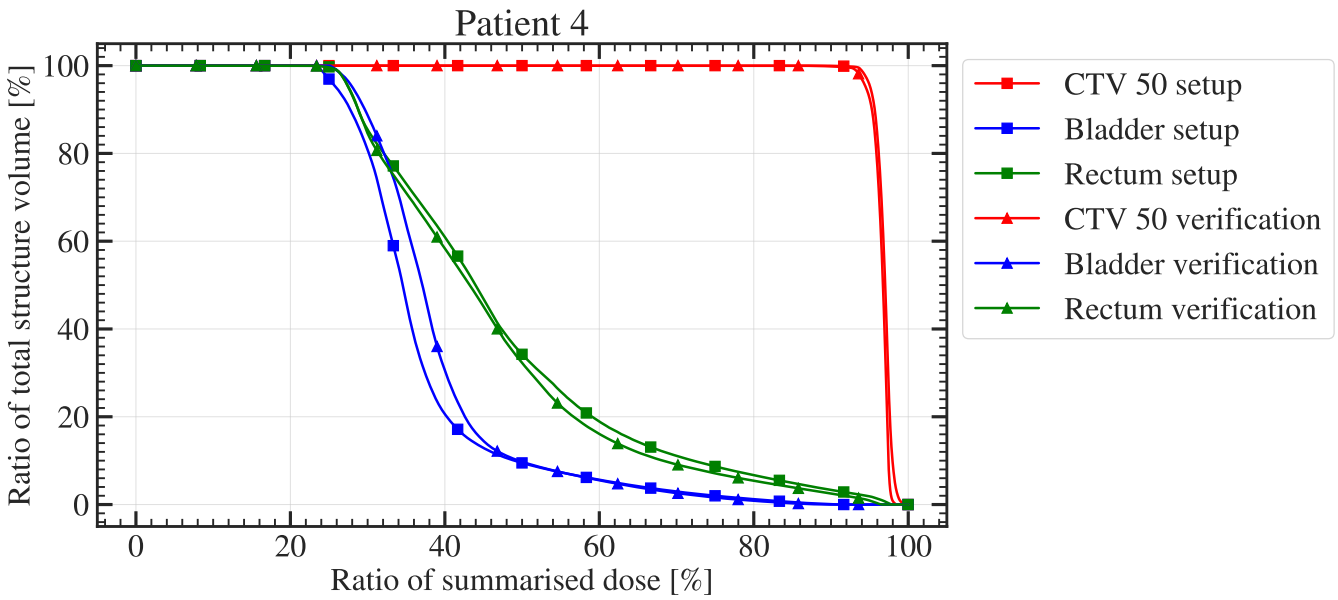

Figure 36

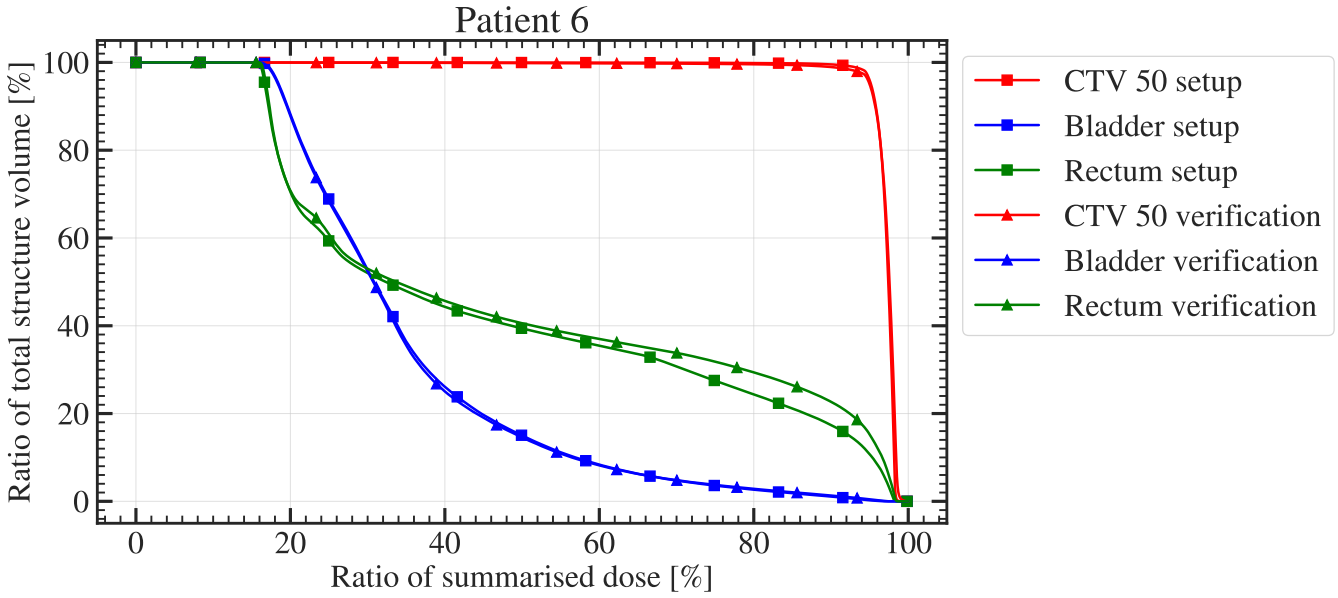

Figure 37

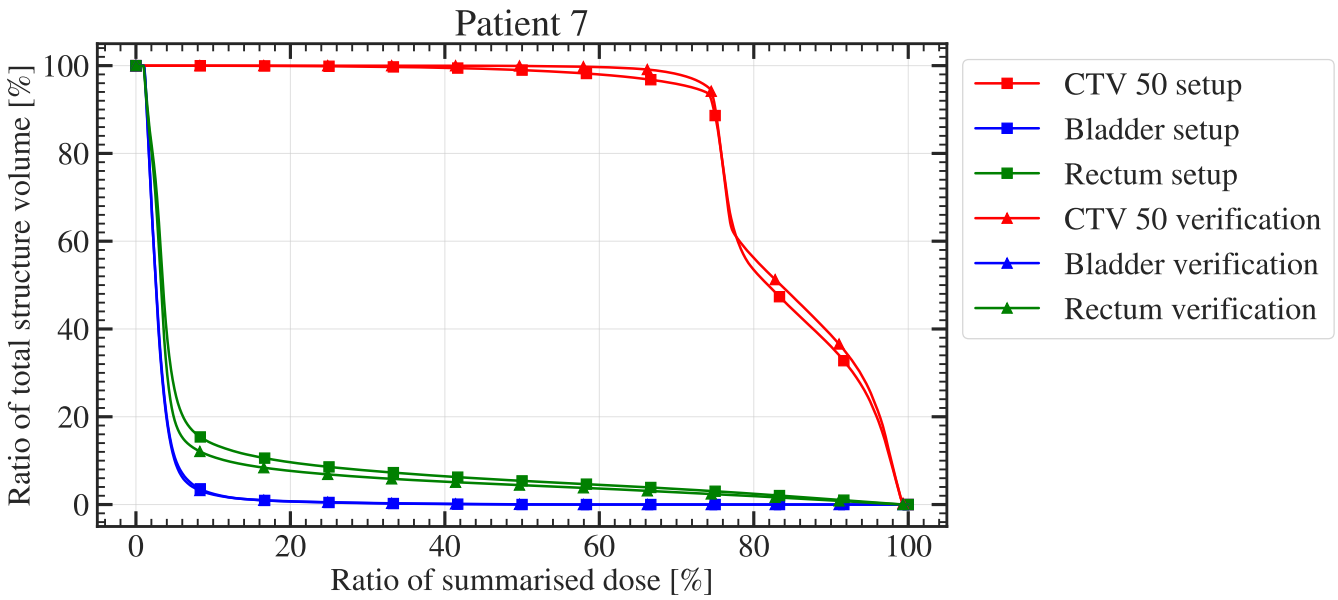

Figure 38

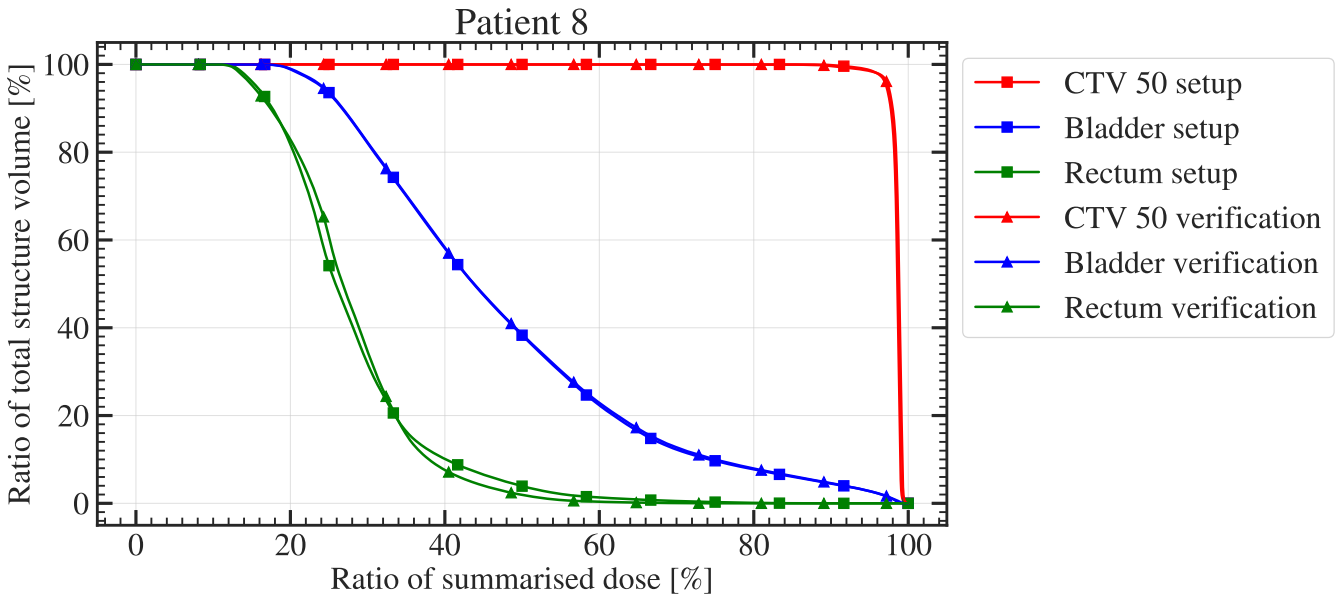

Figure 39

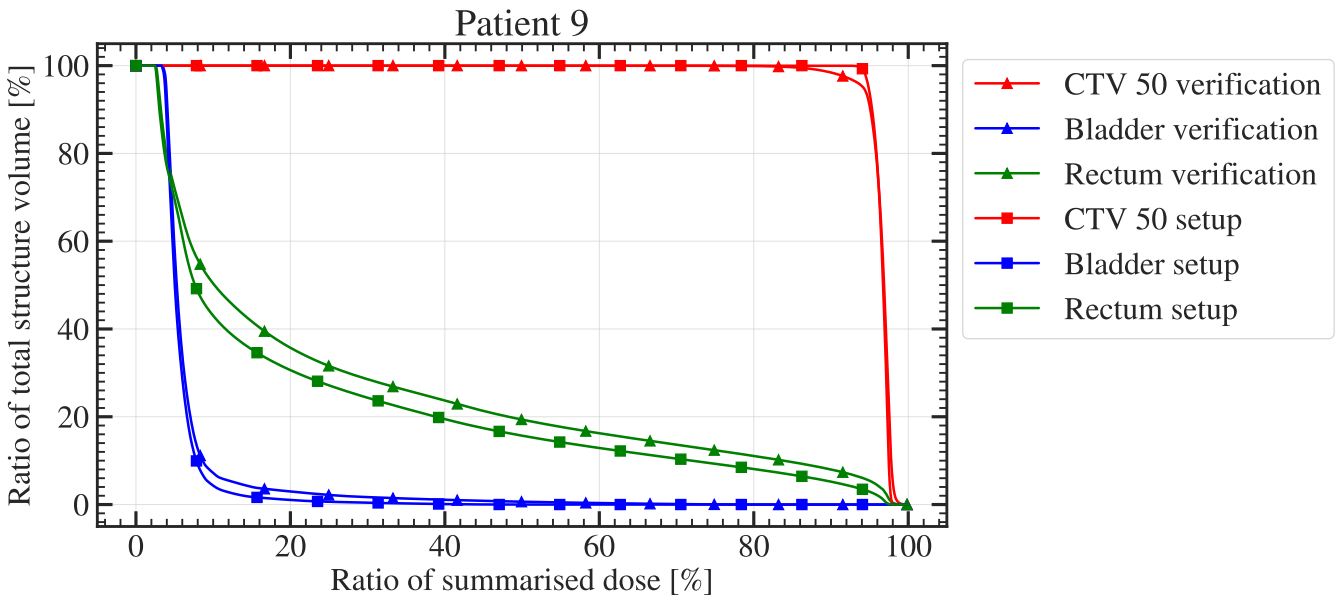

Figure 40

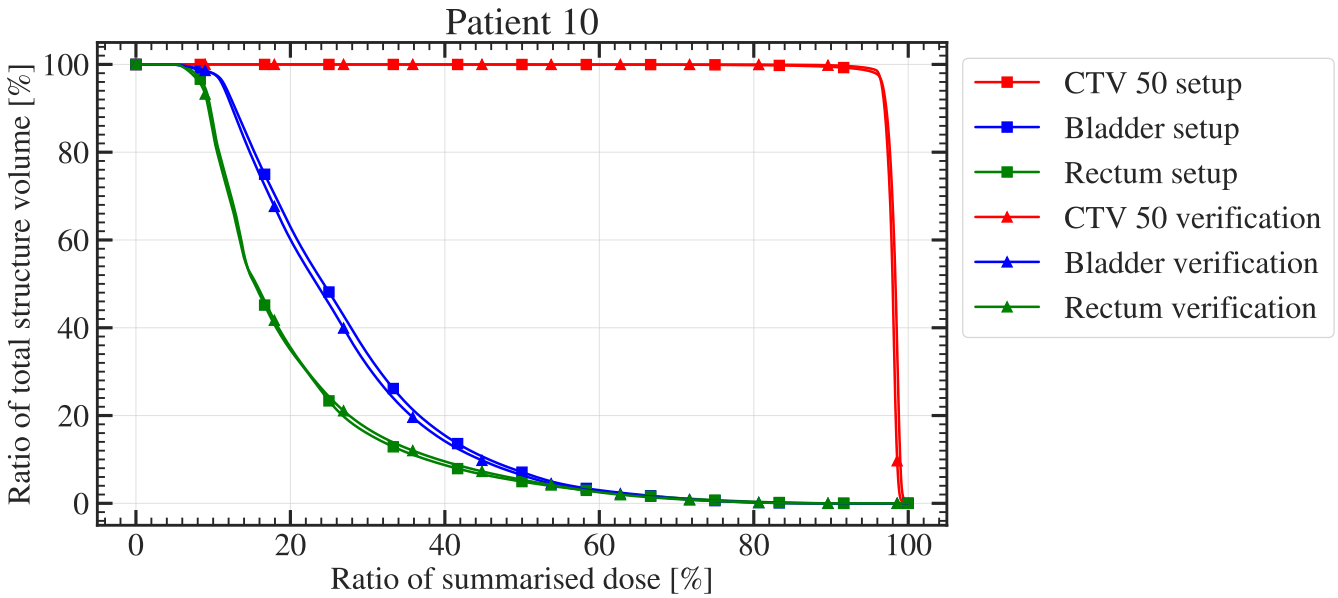

Figure 41